SLAC – PUB – 3478
October 1984
T

THE t–EXPANSION AND $SU(2)$ LATTICE GAUGE THEORY*

DAVID HORN,† ‡ MAREK KARLINER‡ AND MARVIN WEINSTEIN

Stanford Linear Accelerator Center

Stanford University, Stanford, California, 94305

Submitted to *Physical Review D*

* Work supported by the Department of Energy, contract DE – AC03 – 76SF00515.
† Permanent address: School of Physics and Astronomy, Tel-Aviv University, Tel-Aviv, Israel.
‡ Work supported in part by the U.S.–Israel Binational Science Foundation.

ABSTRACT

This paper presents the results obtained by applying the t-expansion to the case of an $SU(2)$ lattice gauge theory in 3+1–space time dimensions. We compute the vacuum energy density, specific heat, string tension σ, mass of the lowest lying 0^{++}-glueball M and the ratio $R = M^2/\sigma$. Our computations converge best for the energy density, specific heat and R, and these quantities exhibit behavior which agrees with what we expect on general grounds and what is known from Euclidean Monte Carlo calculations. In particular we see a broad lump in the specific heat and determine $\sqrt{R}$ to be $\sqrt{R} = 3.5 \pm .2$, a value which lies in the ballpark of values obtained from Monte Carlo calculations. Our direct computations of the mass of the 0^{++} glueball and string tension cannot be easily compared to the results of Monte Carlo calculations, but appear to be consistent with what one would expect.

1. INTRODUCTION

We present calculations of the ground state energy density, $\mathcal{E}$, the string tension, σ, and the mass of the lowest lying 0^{++} glueball, M, for the case of a pure SU(2) gauge theory in 3+1 dimensions. These calculations make use of the *t-expansion*, a non-perturbative calculational tool recently introduced by D. Horn and M. Weinstein[1] and applied to the study of simple lattice spin models. The purpose of this paper is to show how this technique works for an interesting theory in 3+1–space-time dimensions. In addition to the vacuum energy density, string tension and 0^{++} mass we also calculate the specific heat and the ratio $R = M^2/\sigma$. The quantity R is of interest because, on general grounds, R is expected to go to a constant as $g^2 \to 0$ well before either M or σ exhibits perturbative scaling. Consistent with our expectations we find the vacuum energy density, specific heat and R can be extrapolated to the weak coupling regime with small errors; however, the mass of the 0^{++} and the string tension are subject to larger uncertainties. In addition, we find that the specific heat peaks in the turnover region between strong and weak coupling. This result is consistent with the behavior observed in Monte Carlo calculations[2].

2. $SU(2)$:THE t–EXPANSION IN THE STRONG COUPLING BASIS

2.1 FUNDAMENTALS

The t-expansion is a method which can be applied to arbitrary quantum systems defined by a Hamiltonian, H. Underlying the t-expansion is the notion that if $|\psi_0\rangle$ is a state having a finite overlap with the ground-state, then the one

parameter family of states

$$|\psi_t\rangle = \frac{1}{\langle\psi_0| e^{-tH} |\psi_0\rangle^{1/2}} e^{-tH/2} |\psi_0\rangle \tag{2.1}$$

contracts onto the ground state of H as $t \to \infty$. From this it follows that the function

$$E(t) = \frac{\langle\psi_0| He^{-tH} |\psi_0\rangle}{\langle\psi_0| e^{-tH} |\psi_0\rangle} \tag{2.2}$$

tends to the ground-state energy in the same limit. The key result of Ref. 1 is that $E(t)$ can be written as

$$E(t) = \sum_{n=0}^{\infty} \frac{(-t)^n}{n!} \langle H^{n+1}\rangle^c, \tag{2.3}$$

where $\langle H^{n+1}\rangle^c$ is defined recursively by

$$\langle H^{n+1}\rangle^c = \langle\psi_0| H^{n+1} |\psi_0\rangle - \sum_{p=0}^{n-1} \binom{n}{p} \langle H^{p+1}\rangle^c \langle\psi_0| H^{n-p} |\psi_0\rangle . \tag{2.4}$$

Equations (2.3) and (2.4) lead to an expansion of the function $E(t)$ as a power-series in the auxiliary variable t. The method suggested in Ref. 1 for exploiting this expansion is to form Padé approximants to the series in t and use them to evaluate the asymptotic value of $E(t)$. Experience indicates that there is a best way in which to reconstruct such functions from their Padé approximants, and we will discuss this issue in the next chapter.

2.2 THE HAMILTONIAN

The theory we will study is the 3+1–dimensional $SU(2)$ lattice gauge theory defined by the Kogut-Susskind Hamiltonian

$$H = \frac{g^2}{2}\Big[\sum_{\ell} \vec{E}_{\ell}^{\,2} + x\sum_{p}(2 - tr\, U_p)\Big], \tag{2.5}$$

where g is the coupling constant and $x \equiv 4/g^4$. The link operators $\vec{E}_\ell$ and U_ℓ which appear in (2.5) are conjugate quantum variables satisfying the commutation relations

$$\Big[E_\ell^a, U_{\ell'}\Big] = \frac{\sigma^a}{2} U_\ell \delta_{\ell\ell'}. \tag{2.6}$$

Intuitively, the operator E_ℓ^a is the *color electric flux* operator associated with the link ℓ, and $tr\, U_p$ is the magnetic flux operator associated with the plaquette p. The operator U_p is defined to be

$$U_p = U_1 U_2 U_3^{-1} U_4^{-1}, \tag{2.7}$$

where the product of the link operators U_ℓ is taken in the counterclockwise direction. For the case of the $SU(2)$ gauge theory the operator $tr\, U_p$ is Hermitian. In carrying out explicit computations it is useful to work with the operator

$$\overline{H} = \sum_{\ell} \vec{E}_{\ell}^{\,2} - x\sum_{p} tr\, U_p \tag{2.8}$$

which is related to (2.5) by an overall multiplicative and additive constant.

2.3 THE TRIAL STATE

For the computations presented in this paper the state $|\psi_0\rangle$ is taken to be $|0\rangle$, the ground-state of the strong coupling Hamiltonian. This state is defined by the conditions

$$\vec{E}_\ell \, |0\rangle = 0 \, . \tag{2.9}$$

The energy-function we calculate is

$$E(t, g^2) = \frac{\langle 0| \, H \, e^{-t\overline{H}} \, |0\rangle}{\langle 0| \, e^{-t\overline{H}} \, |0\rangle}, \tag{2.10}$$

which is equivalent to making the change $t \to 2t/g^2$ in (2.1), (2.2) and (2.3).

2.4 THE STRING TENSION

In order to compute the string tension for the $SU(2)$ gauge theory we begin by calculating the difference between the ground-state energy of the sector with a string of length L and the sector without any string. The tension, $\sigma(t, g^2)$, is defined by dividing this difference by the length, L, of the string and taking the limit $L \to \infty$. Thus to calculate $\sigma(t, g^2)$ we compute

$$\sigma(t, g^2) = \lim_{L \to \infty} \frac{1}{L} \left[\frac{\langle 0| \, S^\dagger H \, e^{-t\overline{H}} S \, |0\rangle}{\langle 0| \, S^\dagger e^{-t\overline{H}} S \, |0\rangle} - E(t, g^2) \right] \tag{2.11}$$

where the operator S creates a straight infinite string along one axis; i.e.,

$$S = \prod_{\ell=(-\infty,0,0)}^{(\infty,0,0)} U_\ell \, . \tag{2.12}$$

2.5 THE 0^{++} MASS

One can compute the mass of the lowest lying 0^{++} state from the series for the vacuum energy. The way this is done is to show that the function $M(t)$, defined as

$$M(t) \equiv -\frac{g^2}{2}\frac{\partial}{\partial t}\ln\Big(-\frac{\partial E(t)}{\partial t}\Big) \tag{2.13}$$

tends to the mass of the lowest lying 0^{++} state as $t \to \infty$.

To prove this result we begin by considering the state

$$|\omega_t\rangle = H\,|\psi_t\rangle - \langle\psi_t|\,H\,|\psi_t\rangle\,|\psi_t\rangle\,. \tag{2.14}$$

By construction $|\omega_t\rangle$ is orthogonal to the state $|\psi_t\rangle$ for all values of the parameter t. Since the state $|\psi_t\rangle$ contracts onto the lowest lying state having a non-vanishing overlap with the initial state $|\psi_0\rangle$, i.e. the vacuum, it follows that the state obtained by normalizing $|\omega_t\rangle$ contracts onto the lowest lying excitation having the same quantum numbers as the vacuum. With this in mind we only need to show that

$$M(t) = \frac{\langle\omega_t|\,H\,|\omega_t\rangle}{\langle\omega_t|\omega_t\rangle} - \langle\psi_t|\,H\,|\psi_t\rangle\,. \tag{2.15}$$

Direct substitution of the definition of $|\omega_t\rangle$ yields

$$M(t) = \frac{\langle\psi_t|\,H^3\,|\psi_t\rangle - 3\,\langle\psi_t|\,H^2\,|\psi_t\rangle\,\langle\psi_t|\,H\,|\psi_t\rangle + 2\,\langle\psi_t|\,H\,|\psi_t\rangle^3}{\langle\psi_t|\,H^2\,|\psi_t\rangle - \langle\psi_t|\,H\,|\psi_t\rangle^2} \tag{2.16}$$

Since we used $\overline{H}$ in order to define $|\psi_t\rangle$ and $E(t)$ it follows that

$$E(t) \equiv \frac{\langle\psi_0|\,He^{-(2t/g^2)H}\,|\psi_0\rangle}{\langle\psi_0|\,e^{-(2t/g^2)H}\,|\psi_0\rangle}. \tag{2.17}$$

Differentiating (2.17) with respect to t yields the desired equality.

Given this result it is obvious that having computed the series in t for the string tension, $\sigma(t)$, and $M(t)$ one also has a series for

$$R \equiv \frac{M(t)^2}{\sigma(t)}. \tag{2.18}$$

Obviously, the same techniques for forming Padé approximants to the ground state energy density can be applied to the series for $\sigma(t)$ and $R(t)$ in order to reconstruct their values in the limit $t \to \infty$.

2.6 THE COMPUTATION

The technique developed in Ref. 1 allows us to construct $E(t, g^2)$ as a double power-series in t and g^2. The coefficients associated with fixed powers of t are the connected matrix-elements of $\overline{H}$:

$$E(t, g^2) = \frac{g^2}{2} \sum_n \frac{(-t)^n}{n!} \langle \overline{H}^{n+1} \rangle^c + \frac{4}{g^2} N_p \ , \tag{2.19}$$

where N_p is the number of plaquettes associated with the spatial lattice. The vacuum energy density is defined to be

$$\mathcal{E}(t, g^2) = \frac{1}{N_p} E(t, g^2), \tag{2.20}$$

in the limit $N_p \to \infty$. Hence, dividing (2.19) by N_p we obtain an expression for the ground-state energy-density as a Taylor series in t and g^2 or t and $x = 4/g^4$. The relation of this two-parameter expansion to conventional strong-coupling perturbation theory was established in Ref. 1.

As discussed in Ref. 1 the connected coefficients appearing in the formula for $E(t, g^2)$ are computed by restricting attention to *connected diagrams*. One

systematic way to construct the relevant diagrams is to begin by constructing all connected diagrams generated by application of the potential term $(x \sum tr\, U_p)$ to the strong coupling state, as one would do in the perturbation expansion, and then *decorating* the resulting graphs by inserting arbitrary powers of the electric field terms, $\vec{E}_\ell^2$, onto the links appearing in these diagrams. Straightforward computation of connected coefficients to order t^6, or $\overline{H}^7$, leads to the result,

$$\begin{aligned}\mathcal{E} = \frac{4}{g^2} + g^2 t x^2\Big(-\frac{1}{2} + \frac{3t}{4} - \frac{3}{4}t^2 + \frac{9}{16}t^3 - \frac{27}{80}t^4 + \frac{27}{160}t^5\Big) \\ + g^2 t^3 x^4\Big(\frac{1}{12} - \frac{5t}{24} + \frac{41}{240}t^2 + \frac{23}{144}t^3\Big) \\ + g^2 t^5 x^6\Big(-\frac{1}{12} + \frac{7t}{24}\Big)\,.\end{aligned} \tag{2.21}$$

The same sort of calculation for the sector containing a string, i.e. the computation of powers of $\overline{H}$ between the states $\langle 0|\, S^\dagger$ and $S\,|0\rangle$, leads to the result

$$\sigma = \frac{3}{8}g^2 + g^2 t^3 x^2\Big(-\frac{1}{4} + \frac{t}{2} - \frac{35t^2}{64} + \frac{163}{384}t^3\Big) + g^2 t^5 x^4\Big(\frac{1}{16} - \frac{7t}{64}\Big)\,. \tag{2.22}$$

This computation is simplified by the fact that every connected diagram which does not touch the string contributes in the same way to the vacuum energy and the ground-state energy for the sector with a string, and so it follows that in computing the difference of these energies the contributions of these graphs cancel. Thus, we only need to compute connected diagrams that touch the string. It is worth noting that due to these cancellations, one finds that the series for the tension systematically starts out, for a fixed power of g^2, in a higher order of t than it does in the computation of the vacuum energy.

As pointed out in the preceding sections, the series (2.21) and (2.22) can be used to generate series expansions for the quantities $M(t)$ and R. Note that the

formula for $M(t)$ is obtained by taking two derivatives of $E(t)$, so one needs a series for $E(t)$ out to order t^8 in order to generate a series for the mass which is comparable to our series for the string tension. Fortunately, connected matrix elements of H^n up to $n = 10$ have been calculated by A. Duncan and R. Roskies.[3] We will make use of their results in the sections to follow.

3. PADÉ APPROXIMANTS

3.1 General Remarks

To compute the ground-state energy or string tension we use Padé approximants. These approximants are used to extend the region in t over which our calculations are reliable. The eventual goal is to accurately compute these functions in the limit $t \to \infty$. A problem which faces us is to determine how well this asymptotic value is reconstructed by our technique. Given a long enough series to allow us to form many Padé approximants, the best procedure is to compare the t–dependence of different approximants at the same value of the coupling constant. If, as functions of t, the different approximants lie on one another, then experience tells us that it is reasonable to assume the calculation has converged.

In addition to checking on the reliability of a specific calculation, there is the question of which Padé approximant to use. This becomes particularly important if we attempt to exploit the fact that we are dealing with a double power series in t and g^2, and that we have exact information about the function along the axes $t = 0$ or $g^2 \to \infty$. Given a limited number of terms in the series expansion of the function, some ways of handling this double series will do a better job in reconstructing the function than others.

Methods for generalizing Padé approximants to the case of double power series are discussed in the literature; see the book by George A. Baker Jr. and Peter Graves-Morris[4] for a discussion of Chisholm, Canterbury, Hughes-Jones approximants, etc. In general, we found these techniques difficult to apply and not particularly useful for our problem. A more relevant technique, also discussed in Ref. 4, is the method of differential approximants first introduced by Fisher and Kerr[5] . The method of forming Padé approximants to the derivative of the t-series, which we introduced in Ref. 1, turns out to be a special subcase of the general technique. What is surprising is that, to our knowledge, it is a subcase which has not been discussed in the literature. It is this technique, and simple variants thereof, that we make use of in the next section.

To understand the relationship between this method and the differential approximants introduced by Fisher and Kerr, let us consider the simpler case of a function of a single variable. Begin by assuming we have a power series expansion for a function $f(t)$

$$f(t) = \sum_{j=0}^{N} a_j t^j \,. \tag{3.1}$$

The differential Padé approximant for this function is defined as the solution to the differential equation

$$A(t)\,\frac{df}{dt}(t) + B(t)\,f(t) = C(t) \tag{3.2}$$

where $A(t)$, $B(t)$ and $C(t)$ are polynomials of order M_1, M_2 and M_3 respectively. The coefficients appearing in these polynomials are fixed by substituting (3.1) into (3.2) and requiring that the equation is true to terms of order t^{N+1}. The case where $A(t) = 0$, $B(t)$ is a polynomial of order M and $C(t)$ is a polynomial

of order L reduces to the ordinary $[L/M]$–Padé approximant. If $C(t)$ is chosen to vanish the approximants are called D–log Padé approximants, since in this case (3.2) instructs us to form ordinary Padé approximants to the function

$$\frac{d\log(f)}{dt} = \frac{1}{f(t)}\frac{df}{dt}. \tag{3.3}$$

The method used in Ref. 1 assumes that $B(t)$ vanishes; which amounts to forming ordinary Padé approximants to the function $df(t)/dt$ and then reconstructing $f(t)$ by integration. For convenience we will henceforth refer to this type of approximant as a D–Padé approximant. We choose to use D–Padé approximants because for the class of problems in which we are interested we need to reconstruct the asymptotic behavior of functions whose derivatives vanish rapidly as $t \to \infty$. One reason why we expect the D–Padé approximants to yield more accurate results than the value extracted by forming ordinary $[L/L]$–approximants is that our knowledge of the derivative is accurate near $t = 0$ and becomes worse for increasing values of t; hence, when we reconstruct the function $f(t)$ by integration, the effect of an error in the approximation to df/dt for $t = t_0$ won't show up until value of t significantly greater than t_0. If, as is the case for the functions of interest to us, df/dt vanishes rapidly, then the effects of errors at large values of t will be small. Since the functions we are computing are assumed to take finite limits as $t \to \infty$ we know that df/dt vanishes sufficiently rapidly so that $\int dt\,(df/dt)$ converges. In terms of forming Padé approximants this means that the only restriction on $[L/M]$ values that we use is that $M \geq L + 2$. This points out a second advantage of this technique over the use of diagonal approximants, namely that we can form more approximants to a given series and check for consistency.

Before discussing how to exploit the information coming from a series in two variables, it is worth observing that the general equation (3.2) is equivalent to forming an $[L/M]$–Padé approximant to the power series expansion of the derivative of the function $\bar{f}(t) = f(t)/\lambda(t)$, where $\lambda(t)$ is an integrating factor for (3.2) and satisfies

$$\frac{1}{\lambda(t)}\frac{d\lambda}{dt} = -\frac{B(t)}{A(t)}. \tag{3.4}$$

This method shares with the D–Padé approximants the advantage that it reconstructs the full function of t by integration starting from its exact value at $t = 0$.

3.2 Functions of Two Variables

In trying to exploit the theory of Padé approximants for functions like (2.21) or (2.22), we found that nothing worked better than the basic idea we adopted for functions of a single variable; namely, forming Padé approximants to the derivative of the function and then reconstructing the function by integration. Furthermore, we found that since our series tended to be sparse in the variable $y = 2/g^2$ and dense in t, it proved to be best to always use Padé approximants to reconstruct only the t–dependence of the functions in question. Another reason for proceeding in this way is that by not attempting to use Padé approximants in both variables we do not force the asymptotic behavior of any physical quantity as a function of g^2.

We will proceed as follows: given a series for $f(t, y)$, i.e.

$$f(t,y) = \sum_{i=0}^{N_t}\sum_{j=0}^{N_y} a_{ij}\, t^i y^j \tag{3.5}$$

we differentiate it to obtain

$$\frac{\partial^2 f}{\partial y \partial t}(t,y) = \sum_{i=0}^{N_t} \sum_{j=0}^{N_y} ij\, a_{ij}\, t^{i-1} y^{j-1}. \tag{3.6}$$

Next, we form Padé approximants with respect to the variable t to obtain

$$\bar{f}_{yt}^{[L/M]}(y,t) \tag{3.7}$$

and integrate this with respect to t to obtain

$$\bar{f}_{y}^{[L/M]}(y) = \int_0^\infty dt'\, \bar{f}_{yt}^{[L/M]}(y,t'). \tag{3.8}$$

Finally, we use this approximation to $\partial f/\partial y$ to reconstruct $f(y)$ by integration,

$$f(y) = \int_0^y dy'\, \bar{f}_{y}^{[L/M]}(y') \ . \tag{3.9}$$

We have found that for the class of functions with which we are dealing this is the simplest and best way to proceed.

3.3 What Function Should We Padé ?

Having stated what our general approach to reconstructing physical quantities is, one ambiguity remains; namely, for a given physical quantity is it better to Padé approximate the series for the function itself, or is it better to Padé approximate the series for a function of the function? To be more specific suppose we have reason to believe, as we do in the case of the string tension for a pure gauge theory, that the quantity in question exhibits very rapid variation over

the interesting range of couplings. In this event, we could proceed as we have indicated and construct the derivative of the string tension with respect to y and reconstruct the string tension be integrating in from strong coupling.An alternative to this approach is to rework the series into an expansion for a function of the string tension which is expected to behave more smoothly in g^2 namely[6],

$$-\frac{g}{\beta(g)} = \frac{g^2 \partial\sigma/\partial g^2}{\sigma(g^2)}, \tag{3.10}$$

where $\beta(g)$ is, at weak coupling, expected to behave like the β-function obtained from continuum weak coupling perturbation theory. Given long series expansions we would only be happy if all of the methods agreed with one another. However, if one has only short series, there is every reason to believe that one method will be more accurate than another. In the next section we will apply both methods to the computation of the string tension, 0^{++} mass and the ratio of these quantities and compare the results.

4. DISCUSSION OF RESULTS

In this section we will show that our computations of $\mathcal{E}$, the specific heat $(-d^2\mathcal{E}/dy^2)$, and R show every sign of converging well into the weak coupling region. This is not the case for the quantities σ and M; for these quantities we find that only one Padé approximant is well behaved, and so we are not able to estimate the error for our extrapolation of these quantities to $t = \infty$. We begin with a discussion of the well behaved quantities and then discuss the computations of σ and M.

4.1 COMPUTATION OF $d\mathcal{E}/dy$

We already pointed out that when dealing with a series in two variables, in this case the series for $\mathcal{E}(y,t)$, we find that it is best to form the series for $\partial\mathcal{E}(y,t)/\partial y$, reconstruct the $t \to \infty$ behavior of this function using D–Padé approximants, and then reconstruct $\mathcal{E}(y)$ by integrating this result with respect to y. Figures 1(a), (b) and (c) exhibit curves obtained in this way for a range of $y = 2/g^2$ going from 0 to 3 (i.e., g^2 from 2/3 to ∞). The figures are essentially self explanatory, however there are some features of the pictures which merit some discussion.

First, we observe that second order perturbation theory implies that $d\mathcal{E}(y)/dy$ is a monotonically decreasing function of y. Since the weak and strong coupling expansions tell us that $d\mathcal{E}/dy(0) = 2$ and $d\mathcal{E}/dy(\infty) = 0$, it follows that $d\mathcal{E}/dy(y)$ must be a positive function of y. In figure 1(a) we see a plot of [L/L+2] D–Padé approximants to $d\mathcal{E}/dy$. We display this set of approximants in order to give the reader a feeling for the rate at which they are converging. It is obvious from this set of curves that successively higher values of L lead to curves for $d\mathcal{E}/dy$ which appear to converge rapidly for this range of y. The highest approximant still undershoots and goes negative for $y > 2.2$ ($g^2 < .8$); however it only does so by a small amount, and the Padé approximants appear to be converging to a function which tends to zero from above, in agreement with general expectations. Invoking the exact theorem which tells us that $d\mathcal{E}/dy$ must be positive, we see that our reconstruction of this $d\mathcal{E}/dy$ breaks down for $y \geq 2.1$. We should emphasize that the fact that this function tends to zero is in no way built into our calculation by our use of Padé approximants; in fact, since we only use Padé approximants for the t behavior of a function, there is no particular reason of $d\mathcal{E}/dy$ to go to

a constant as $y \to \infty$.

Another feature of these curves which one should remark upon is that the [2/4] Padé approximant exhibits a pole for value of $y \simeq .6$. It is clear that since this pole occurs in only one Padé approximant it is of no significance, and all it does is make the estimate of $d\mathcal{E}/dy$ in the region of the pole unreliable. In fact, one sees that by the time $y > 1.2$ both the [2/4] and [3/5] Padé approximants agree quite well.

Figure 1(b) shows a similar set of curves, except that now we are plotting $[L/L+3]$ D–Padé approximants. Once again we see that the functions undershoot zero, and one Padé approximant exhibits a spurious pole in y; however, the clear tendency of the set of Padé approximants is to converge to a function which is tending to zero from above.

In figure 1(c) we compare all of the reconstructions of $d\mathcal{E}/dy$ which can be formed from the series for $\mathcal{E}(y,t)$ taken to order t^9. The only restriction on these Padé approximants is that $\partial^2\mathcal{E}/\partial y\partial t$ must be integrable with respect to the variable t. It is our experience that the disagreement among the curves of this type gives a good measure of how well the approximants have converged. Once again we see that the reconstruction of $d\mathcal{E}/dy$ for $y \leq 2.1$ is probably reasonable.

4.2 Computing the Energy Density

In figures 2(a), (b) and (c) we display the results obtained by integrating the previous curves for $d\mathcal{E}/dy$. Note that we have added two additional curves to our plot of the Padé approximants to the energy density, one labelled Pert. Theory and one labelled Mean Plaquette. These two curves are added in order to give the reader something to which to compare our results. The curve labelled Pert.

Theory represents the result one obtains from strong coupling perturbation theory carried out to a comparable order in $1/g^2$; the curve labelled Mean Plaquette represents an exact upper bound on the ground state energy density obtained in ref. 7. Another feature of Fig. 2(a), (b) and (c) requires explanation; namely, that the curves for the energy density go to constants rather than turning down when $d\mathcal{E}/dy$ goes negative. In producing these curves we set $d\mathcal{E}/dy$ to zero after it goes negative for the first time. This procedure allows us to avoid plotting a set of curves which cross one another. This is a reasonable procedure, since we know that when the Padé approximant to $d\mathcal{E}/dy$ becomes negative, the calculation is demonstrably unreliable. It is interesting to examine the behavior of the [2/5] approximant, since the [2/5] approximant to $d\mathcal{E}/dy$ had a pole. This curve exhibits a property which we have generally found to hold, and that is that if we evaluate the integral using a principle value prescription for handling the pole, then we find that the reconstruction of the desired function over most of the range is quite satisfactory.

4.3 The Specific Heat

Euclidean Monte Carlo calculations[2] have shown that there is a peak in the second derivative of the ground state energy density with respect to y, which does not appear to be associated with a phase transition, but seems to occur at about the same value of y at which the string tension turns over. This region is generally believed to mark the crossover between strong and weak coupling behavior. In the Euclidean formalism this second derivative of the free energy with respect to the coupling constant is conventionally referred to as the specific heat, and we have adopted the same terminology for the analagous quantity $-d^2\mathcal{E}/dy^2$.

We do this because the ground state energy density of the Hamiltonian version corresponds to the free energy of the Euclidean version of the theory.

In figure 3 we exhibit a plot of the specific heat, $-d^2\mathcal{E}/dy^2$, for various D–Padé approximants. The dashed curves depict the results obtained by differentiating $[L/(5-L)]$ D-Padé approximants to $d\mathcal{E}/dy$ for $L = 0, 1$; the solid curves depict the same function as obtained from $[L/(8-L)]$ D–Padé approximants for $L = 0, 1, 2, 3$. Clearly, both sets of curves exhibit a peak in the specific heat in the region $y \simeq 1$. An important feature of this set of curves is that as one goes to higher order in the t–expansion (i.e., from the $[L/(5-L)]$ to $[L/(8-L)]$ D–Padé approximants) the peak in the specific heat becomes somewhat lower and broader. This is of course just the opposite of what would occur if this peak indicated the existence of a phase transition.

4.4 The Ratio R

The last quantity whose t-expansion is expected to have a convergent set of D–Padé approximants into the weak coupling region is the ratio R. Unfortunately, since the series for the string tension σ only goes out to order t^6, the series for R is not as lengthy as the one for the energy density. To give a feeling as to how successive D–Padé approximants converge we can only plot [0/M] approximants for increasing values of M. These curves are presented in figure 4(a) and (b). Clearly, all of these curves exhibit a marked turnover at values of $g^2 \simeq 2$ (i.e., $y \simeq 1$) which coincides with the region in which the specific heat exhibits a peak. The difference between the curves in figure 4(a) and figure 4(b) is that the first set of curves are obtained by forming D–Padé approximants to the series for R itself, whereas the second set of curves are obtained by forming D–Padé

approximants to dR/dy and then integrating. We include both sets of curves to give the reader some feeling for how the two techniques differ. In figure 4(c) we display the curves corresponding to the $[L/5-L]$ D–Padé approximants obtained in both ways. From this plot we see that all of the different ways of computing this quantity are consistent to ten percent in the region $g^2 > 1.2$.

Finally, in figure 5 , obtained from fig. 4(c), we plot the square root of R as a function of g^2. From this figure we estimate the ratio $M(0^{++})/\sqrt{\sigma}$ to be 3.5 ± 0.2. In principle this quantity, being a dimensionless ratio of physical quantities can be directly compared to the same quantity as computed using Euclidean Monte Carlo techniques. In a Monte Carlo calculation the glueball mass and the string tension can only be computed separately. In order to make the comparison we have searched the recent literature reporting Monte Carlo computations[8–14] of $M(0^{++})$ and σ. The Monte Carlo computations were done using either standard single plaquette action or its various possible modifications [9,10,13]. In principle, if universality holds and if the computations are really in the scaling region, then all of the Monte Carlo computations should agree. However, even in the case of the single plaquette action the results quoted in the literature span a considerable range. The values of $\sqrt{\sigma}$ vary[9] from 69 Λ_L to 52 Λ_L, depending on the method used to extract the string tension. In the same way, the values quoted for $M(0^{++})$ vary[8,9] from $(190 \pm 30)\Lambda_L$ to $(166 \pm 15)\Lambda_L$. Hence, the values of $\sqrt{R}$ which one obtains by combining these results vary from 3.7 ± 0.6 to 2.4 ± 0.2. The extended action computations yield $\sqrt{R}$ ranging from 2.8 ± 0.3[13] to 3.6 ± 0.7[9]. The central value of R obtained from Monte Carlo calculations is in good agreement with our result. However, the rather large error bars on the MC data should be kept in mind.

4.5 The Mass and The String Tension

Now, let us turn to a discussion of quantities which are not quite as well behaved; namely, the glue-ball mass and the string tension. Referring back to (2.22), the series for $\sigma(t, g^2)$, we see that the first t-dependent term occurs in order t^3. Since we have only calculated to order t^6, this means that only the [2/3] D–Padé approximant to this quantity can be formed. However, this approximant does not fall off rapidly enough in t to allow us to extrapolate to $t \to \infty$. For this reason we cannot calculate the string tension directly from (2.22). This presents us with no insurmountable difficulty since we have a full series for the mass of the 0^{++} containing all terms out to t^7. Thus we can compute M or M^2 by our techniques and then reconstruct the string tension by dividing the result by $R(t = \infty, g^2)$. We will show that although one can obtain apparently striking results for the string tension, the comparison of different ways of computing the same quantity is not as stable as the behavior seen for the quantities we have already discussed. We believe that this occurs because our series for the mass is a tad too short, and it mirrors the fact that our series for the string tension has gaps.

Let us begin by showing that only one of the possible highest order D–Padé approximants leads to a reasonable behavior for the quantity M. Figure 6 (a) shows the behavior for mass of the 0^{++} state as reconstructed using the [0/6], [1/5] and [2/4] D–Padé approximants evaluated for a typical value of t, $t = 2$. The point to notice is that the [0/6] and [1/5] approximants lie above the prediction of strong coupling perturbation theory, even for large values of the coupling constant. This is clearly incorrect and reflects the behavior of only the lowest order terms in the t-expansion for the mass of the 0^{++} state. Somehow, the [0/6]

and [1/5] approximants force the t-dependence of the mass to fall too rapidly for the higher order terms in the t-expansion to play a role for any value of t. This leaves us with only one useful approximant, and no way of establishing a reliable estimate of the errors to be associated with the calculations of the mass. Nevertheless, it is instructive to see what results can be obtained from this approximant.

In figure 6(b) we plot a set of curves showing how the reconstruction of M from the [2/4] D–Padé approximant depends upon t. Note that in obtaining this set of curves we have not yet made use of the technique of first computing the derivative of M with respect to g^2 and then reconstructing the function of interest by integration. There are two salient features of this set of curves. First, we see that for small values of g^2 and quite small values of t the mass goes negative, indicating that the results cannot be trusted in this region. This is of course totally consistent with the results obtained for all other quantities and is no surprise. Second, we see a sharp turnover developing for $g^2 \approx 1.6$ which is the region in which all of the other calculations seem to signal the onset of the crossover region between strong and weak coupling. This dip can be seen to deepen with increasing values of t until finally, for $t \geq 2.3$, M goes negative, clearly signaling the breakdown of the approximation. This breakdown occurs before the t-dependence of the reconstruction has slowed significantly, and so we cannot use it to reconstruct the $t \to \infty$ value of $M(t, g^2)$. We can, however, use it at finite values of t and compare the results obtained to what is expected from weak coupling perturbation theory.

One way to compare these calculations of M to continuum perturbation the-

ory is to study the behavior of the function

$$-\frac{g}{\beta_{M^2}(g)} \equiv \frac{g^2 \partial M^2/\partial g^2}{M^2(g^2)}. \tag{4.1}$$

On dimensional grounds, since we believe that lattice Q.C.D. is an asymptotically free theory with no intrinsic scale, this quantity should exhibit the same scaling behavior as the string tension and should therefore go over to $-g/\beta_c(g)$; where by $\beta_c(g)$ we mean the usual continuum β function. In figure 7 we plot the curves for $\beta_{M^2}(g)$ obtained from figure 6(b) and compare it to the behavior expected from the leading term in weak coupling perturbation theory. We see from these curves that the dip in the mass corresponds to the point at which the function $\beta_{M^2}(g)$ (obtained by numerical differentiation of the [2/4] D–Padé approximant to M) approaches the weak coupling curve. This happens for $t \sim 2$. We hasten to point out, however, that the fact that these curves touch at this value of t does not really mean that this is a correct value of t at which to stop our extrapolation. The truth is that in this case we really have no grounds for reliably choosing to stop at any finite value of t. One way to see how one can deceive oneself by proceeding in this way is to divide M^2 for various values of t by a typical curve for R, say $R_{[1/4]}$, in order to obtain curves for the string tension. Figure 8 shows the results of doing this for the curves shown in figure 6 and compares the result to both the leading order prediction from strong coupling $\sigma_0 = (3/8)g^2$, and to the result obtained by carrying the series out to $1/g^{16}$ which we took from a paper by Kogut and Shigemitsu[15]. It turns out that for $t \geq 2$ the string tension computed in this way departs significantly from perturbation theory in a region of g^2 in which we expect strong coupling perturbation theory to be quite accurate. Computing both the β function and the string tension in a region

in which there is still significant t dependence leads to the result that t can be chosen so as to either make the string tension agree with the results of strong coupling perturbation theory for $g^2 \geq 2$, or the β function can be made to touch the weak coupling line; both things cannot be done at the same time.

Having discussed the dangers associated with trying to draw firm conclusions from a calculation which is exhibiting significant t dependence, we now turn to the question of what happens if we use D–Padé approximants in t to reconstruct M from its derivative with respect to g^2. In fact, we will discuss the results of proceeding in a slightly different way in order to make the comparison with weak coupling perturbation theory most straightforward. In analogy with fig 6(b), in figure 9 we plot the [2/4] result obtained by using the D–Padé method to directly reconstruct the function $-g/\beta_{M^2}(g)$ from its t–series. The curves in figure 9 are for $t = .5, 1, 2, 1000$. Clearly the D–Padé reconstruction of this function goes asymptotic for $t \approx 2$. We have found a similar behavior for the energy density $\mathcal{E}$ and the ratio R. Note that although the β function computed in this way never does make contact with weak coupling perturbation theory it appears to be attempting to become a straight line for $g^2 < 2$. Amusingly, the slope of this line appears to parallel the weak coupling line; although the significance of this result is problematical.

In figures 10 and 11 we show the plots of $M(g^2)$ and $\sigma(g^2)$ which we reconstruct from this computation of the β-function. The reconstruction is done as follows. From eq. (4.1) we obtain

$$M^2_{[L/M]}(g^2) = M^2_0(g^2_{max}) \exp\left(- \int_{g^2_{max}}^{g^2} \frac{dg^2}{g^2 \beta_{[L/M]}} \right) \tag{4.2}$$

where $\beta_{[L/M]}$ stands for [L/M] Padé approximant to $\beta(g)/g$, M_0 is the leading term strong coupling result, $M_0 = 3g^2/2$ and $g^2_{max} = 4$. String tension σ is then obtained from M^2 by dividing by a typical value of R, $R_{[1/4]}$. In fig. 11 the line $\sigma_0 = (3/8)g^2$ and the strong coupling curve, taken from ref. 15, are once again added to guide the eye. Obviously, for this calculation there is even less t dependence in the string tension than in the β function. We see that the reconstructed curves remain close to the strong coupling result for $g^2 > 2$. In addition, despite the fact that the β function never quite reaches the weak coupling curve, the string tension essentially vanishes by the time we reach $g^2 \approx 1.4$. This result, if reliable, would seem to bode well for the computation of quantities like hadron masses, etc.; since, it would imply that one need not know too much about what is going on for very small values of g^2 in order to do a reasonable job in computing ratios of masses.

5. SUMMARY

We have described the application of the t–expansion to an $SU(2)$ lattice gauge theory in 3+1 space-time dimensions. Both the computations of the vacuum energy density and the ratio R appear to stabilize for $g^2 > 1$, where the criterion for stability is that various Padé approximants for these quantities agree reasonably well. The value for R which we determine in this way seems to agree quite well with the best available Euclidean Monte Carlo calculations. In addition to these results we directly compute a β function for the mass of the 0^{++} glueball and show that the direct computation of $-g/\beta_{M^2}$ quickly becomes asymptotic in t and tends to exhibit the qualitative behavior one expects from weak coupling perturbation theory. Since, however, we only have one good D–Padé approxi-

mant to $\beta_{M^2}(g)$ we cannot establish a measure of the error in our calculation of this quantity or the string tension which is derived from it.

It is clear from these results that one must carry the t-expansion out to higher orders in order to obtain the correct behavior of the mass and string tension at weak coupling. However, quantities like R, which should tend to a constant as $g^2 \to 0$, appear to exhibit this sort of scaling behavior for $1 \leq g^2$ even for the series computed out only as far as t^6. This turnover is consistent with that seen in $d\mathcal{E}/dy$, the specific heat and the change in character of the β-function, and so we feel it indicates the presence of a scaling window in the region $1 \leq g^2 \leq 2$. Although numerical predictions of this ratio (and many others) have already been calculated by Monte-Carlo techniques, it should be emphasized that our result is obtained by analytic techniques and would appear to have smaller errors than the corresponding Monte Carlo computations. This, coupled with the fact that adding fermions to this scheme is totally straightforward and merely requires the computation of additional graphs, raises the hope that the t-expansion method will be well suited to the problem of extracting low energy hadron physics from lattice Q.C.D.

ACKNOWLEDGEMENTS

D. Horn would like to thank the Institute for Fundamental Physics of Kyoto University for its hospitality during the time in which some of this work was being done. M. Karliner would like to acknowledge support from Tel-Aviv university in the form of Ph.D. fellowship during the period of this research. We are very grateful to A. Duncan and R. Roskies for making the results of their computation of the moments of H in the strong coupling vacuum available to us. Without

their results for the terms of order H^8 to H^{10} it would have been much harder for us to complete this work. In addition, we would like to thank Tom Banks for many helpful discussions. M. Weinstein would like to extend particular thanks to Tom Banks for forcing him to work on a problem in 3+1 dimensions.

FIGURE CAPTIONS

1. Curves of $d\mathcal{E}/dy$ obtained using the D–Padé technique.

   (a) $d\mathcal{E}/dy$ computed by forming $[L/(L+2)]$–Padé approximants to $\partial^2\mathcal{E}/\partial y\,\partial t$.

   (b) $[L/(L+3)]$–Padé approximants to $d^2\mathcal{E}/dy\,dt$. Note the pole in the [2/5]–Padé approximant.

   (c) Comparison of all $[L/(8-L)]$–Padé approximants in order to show that the different sets of approximants behave similarly when computed to the same order in t.

2. Curves showing the energy density $\mathcal{E}(y)$ obtained by integrating the corresponding $[L/M]$–Padé approximants to $d\mathcal{E}/dy$. Note, that in graphing these curves we have set $d\mathcal{E}/dy$ to zero for all values $y > y_0$, where y_0 is the first value of y for which $d\mathcal{E}/dy$ vanishes.

3. Plot of $-d^2\mathcal{E}/dy^2$ for various D–Padé approximants. Continuous lines correspond to $[L/(8-L)]$ Padés. Dashed lines correspond to $[L/(5-L)]$ Padés.

4. Curves showing the convergence properties of the calculation of the ratio R as a function of g^2.

   (a) $[0/M]$ D–Padé approximants to $R(g^2)$.

   (b) Curves showing $R(g^2)$ obtained by forming $[0/M]$ D–Padé approximants to the series for dR/dy and integrating the resulting expression with respect to y.

   (c) Comparison of all approximants to $R(g^2)$ which make use of the entire available series for dR/dt.

5. A plot of the approximants to $\sqrt{R(g^2)}$ obtainable from the full series in t.

6. (a) Plots of the [0/6], [1/5] and [2/4] Padés of M for t=2 (b) Plots of the t-dependent reconstruction of M using the [2/4] D-Pade directly on the series for M. The plots are for t=.5, 0.8, 2. $M_0 = 3g^2/2$, the leading strong coupling result for M.

7. Curves showing the beta function computed from the M plots of fig. 6 (b). Plot of weak coupling continuum perturbation theory is included for comparison.

8. The string tension reconstructed by dividing the [2/4] D–Padé for M^2 by a typical value of R, $R_{[1/4]}$.

9. Plot of a direct computation of the [2/4] beta function by D-Padéing the series for $-g/\beta(g) = g^2\partial \log M^2/\partial g^2$. Plots are given for t=.5, 1, 2, 1000.

10. Curves showing M reconstructed from the β–functions of Fig. 9.

11. String tension obtained from Fig. 10 by dividing by a typical value of R, $R_{[1/4]}$.

REFERENCES

1. D. Horn and M. Weinstein, *Phys. Rev.* **D30** (1984) 1256.
2. B. Lautrup and M. Nauenberg, *Phys. Rev. Lett.* **45** (1980) 1755.
3. A. Duncan and R. Roskies, private communication.
4. *"Padé Approximants Part II: Extensions and Applications"*, by George A. Baker. Jr and Peter Graves-Morris, Encyclopedia of Mathematics and Its Applications, Vol 14., Addison-Wesley,1981.
5. M. E. Fisher and R. M. Kerr, Phys. Rev. Lett., **39** (1977) 667.
6. J. Kogut, R. B. Pearson and J. Shigemitsu, *Phys. Rev. Lett.* **43** (1979) 484.
7. D. Horn and M. Karliner, *Nucl. Phys.* **B235** (1984) 135.
8. H. Meyer-Ortmans and I. Montvay, DESY preprint DESY 84-034, April 1984.
9. B. Berg, A. Billoire, S. Meyer, C. Panagiotakopoulos, Saclay Preprint Saclay-PhT/84-24; to appear in Commun. Math. Phys.
10. V. Azcoiti and A. Nakamura, *Phys. Lett.* **144B** (1984) 91.
11. B. Berg, A. Billoire, C. Rebbi, *Annals Phys.* **142** (1982) 185; addendum - ibid. **146** (1983) 470.
12. A. Billoire and E. Marinari, *Phys. Lett.* **139B** (1984) 399;
    F. Karsch and C.B. Lang, *Phys. Lett.* **138B** (1984) 176;
    F. Gutbrod and I. Montvay, *Phys. Lett.* **136B** (1984) 411.
13. M. Fukugita, T. Kaneko, T. Niuya, A. Ukawa, *Phys. Lett.* **134B** (1984) 341; erratum - ibid. **137B**(1984) 444.

14. M. Teper, Annecy preprint, LAPP-TH-91, Oct 1983.

15. J. B. Kogut and J. Shigemitsu, *Phys. Rev. Lett.* **45** (1980) 410; erratum - ibid. **45** (1980) 1217.

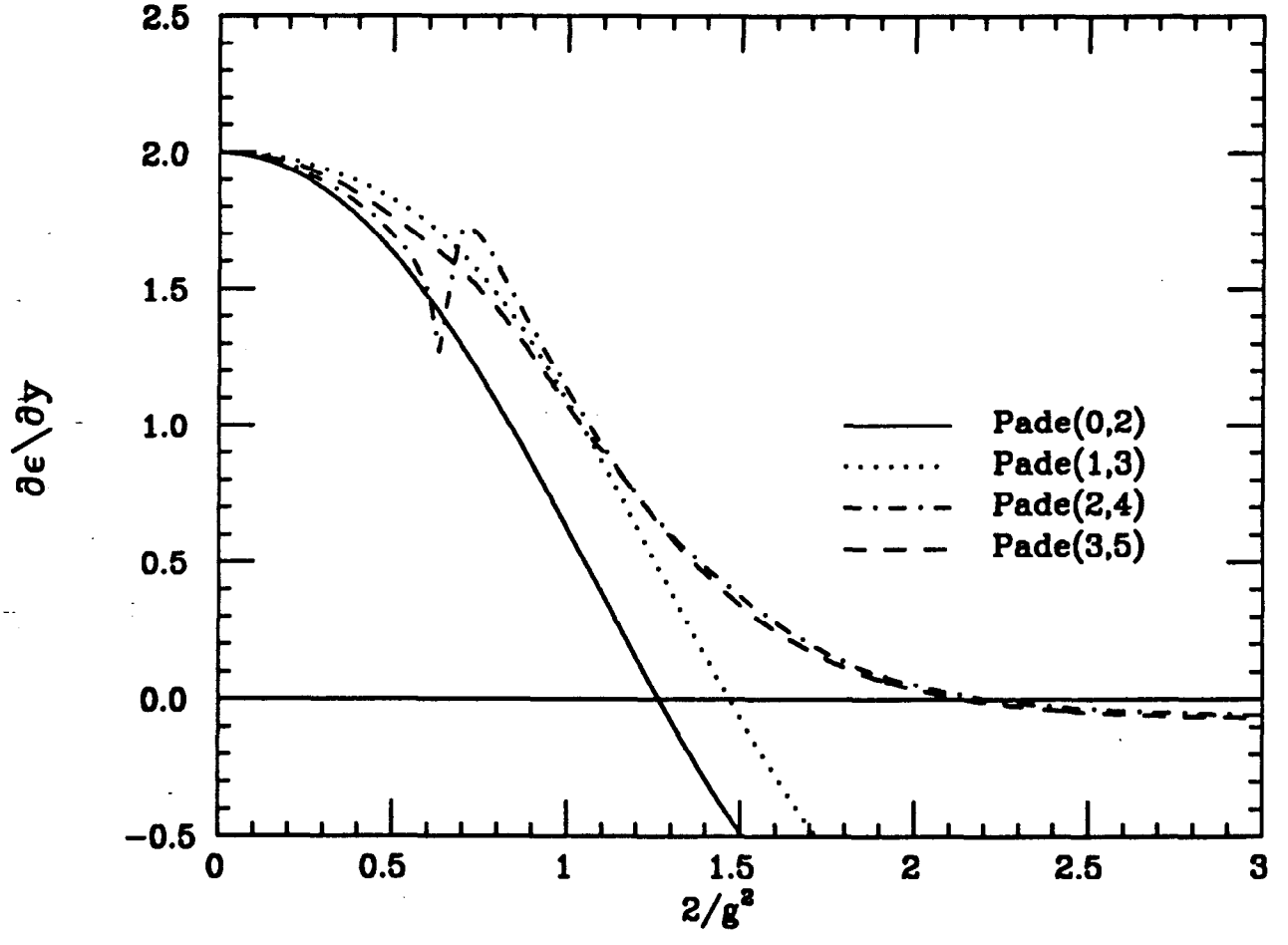

FIG. 1A

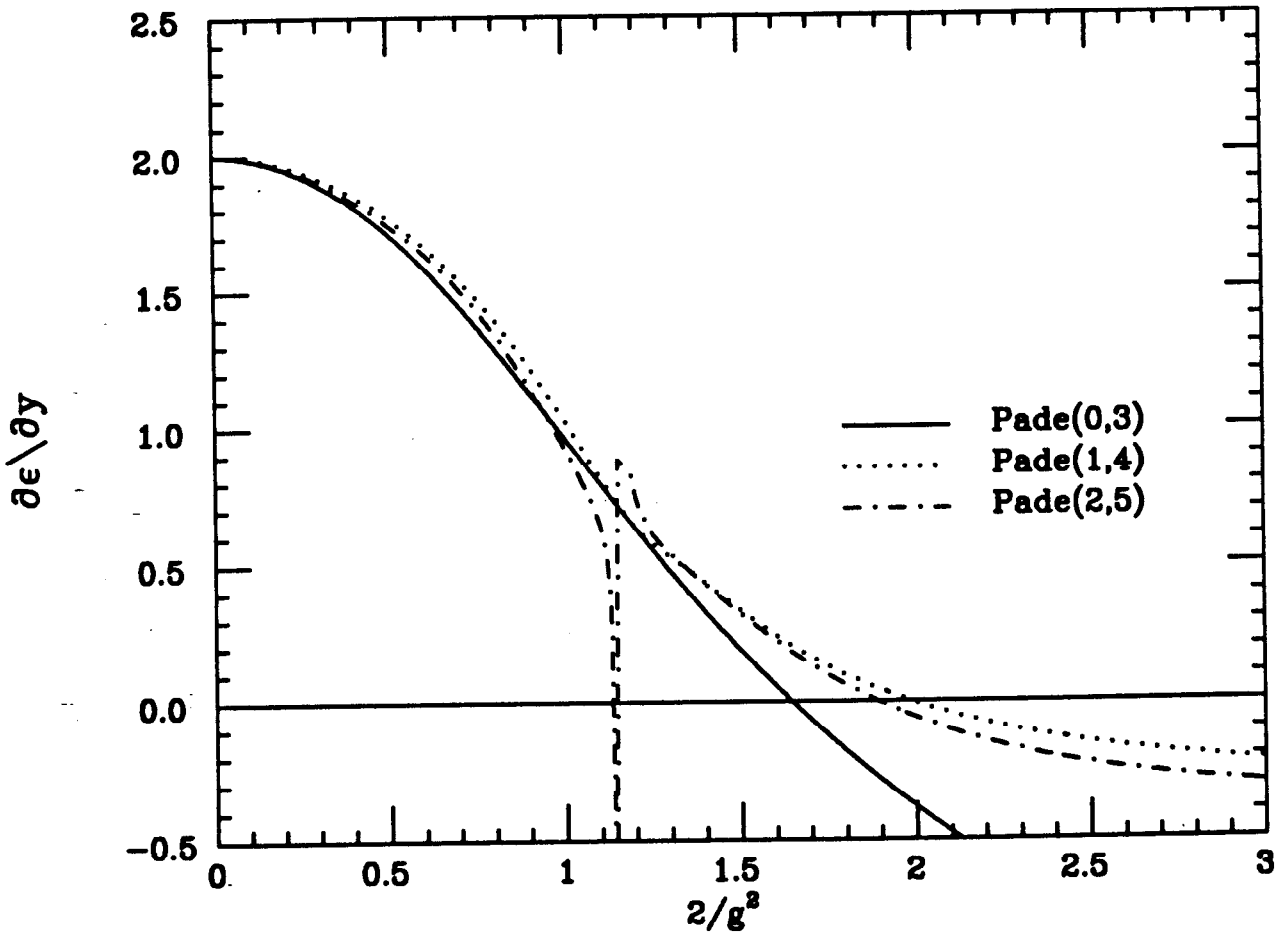
2.5
2.0
1.5
1.0
0.5
0.0
-0.5
0
0.5
1
1.5
2
2.5
3
$\partial\epsilon\backslash\partial y$
$2/g^2$
Pade(0,3)
Pade(1,4)
Pade(2,5)

FIG. 1B

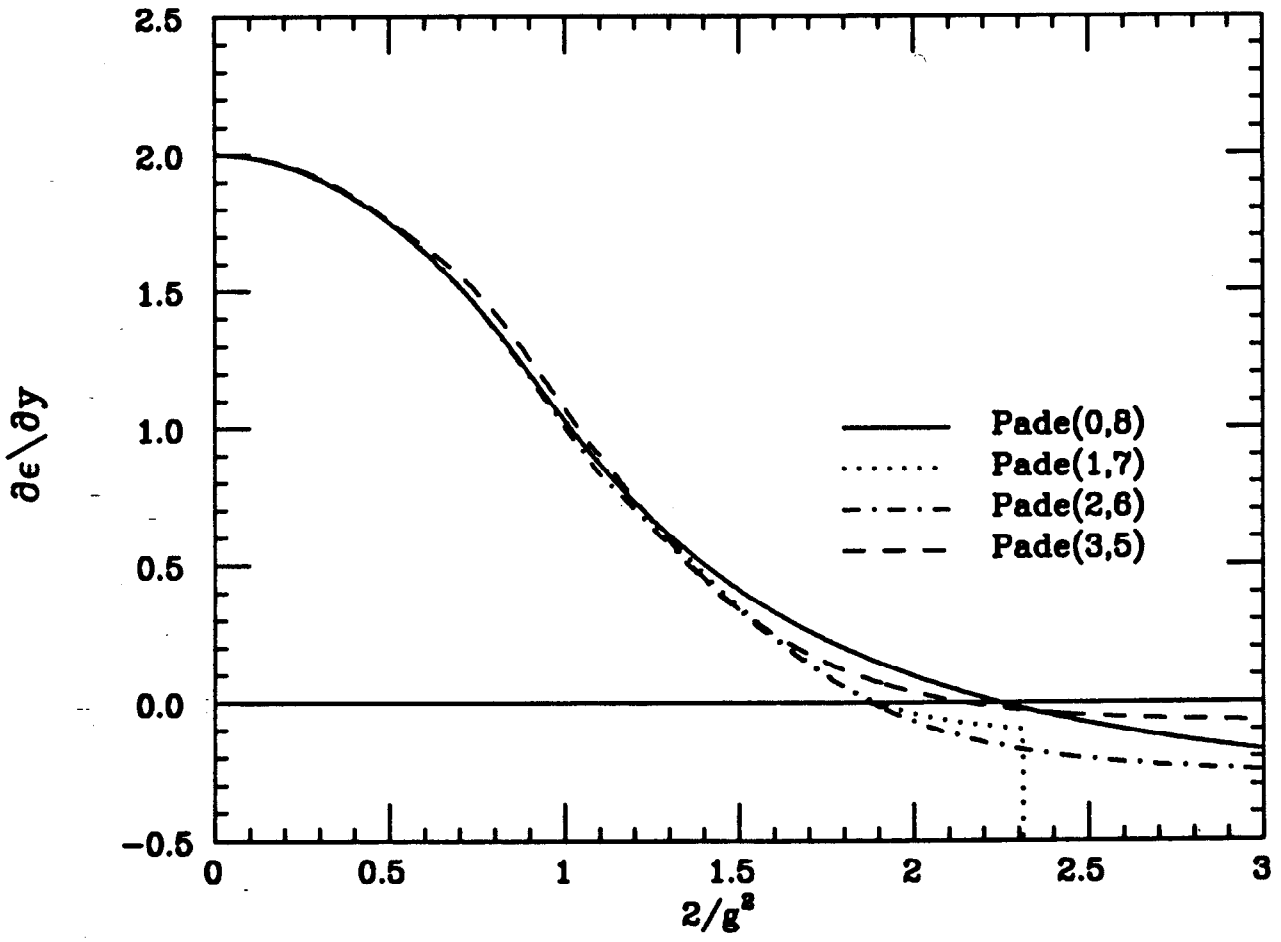
2.5
2.0
1.5
1.0
0.5
0.0
−0.5
0
0.5
1
1.5
2
2.5
3
$\partial\epsilon\backslash\partial y$
$2/g^2$
Pade(0,8)
Pade(1,7)
Pade(2,6)
Pade(3,5)

FIG. 1c

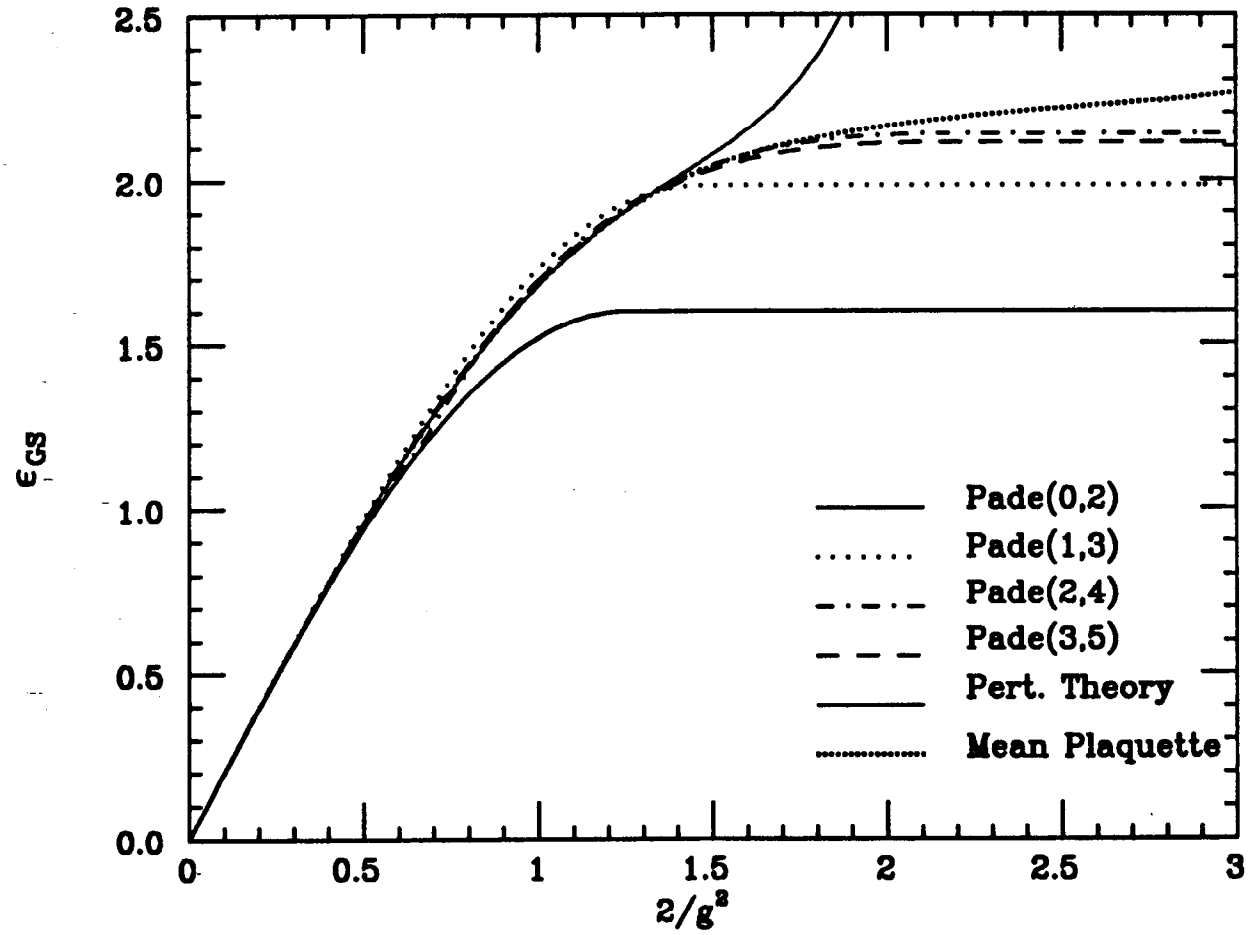
2.5
2.0
1.5
1.0
0.5
0.0
ϵ_{GS}
0
0.5
1
1.5
2
2.5
3
$2/g^2$
Pade(0,2)
Pade(1,3)
Pade(2,4)
Pade(3,5)
Pert. Theory
Mean Plaquette

FIG. 2A

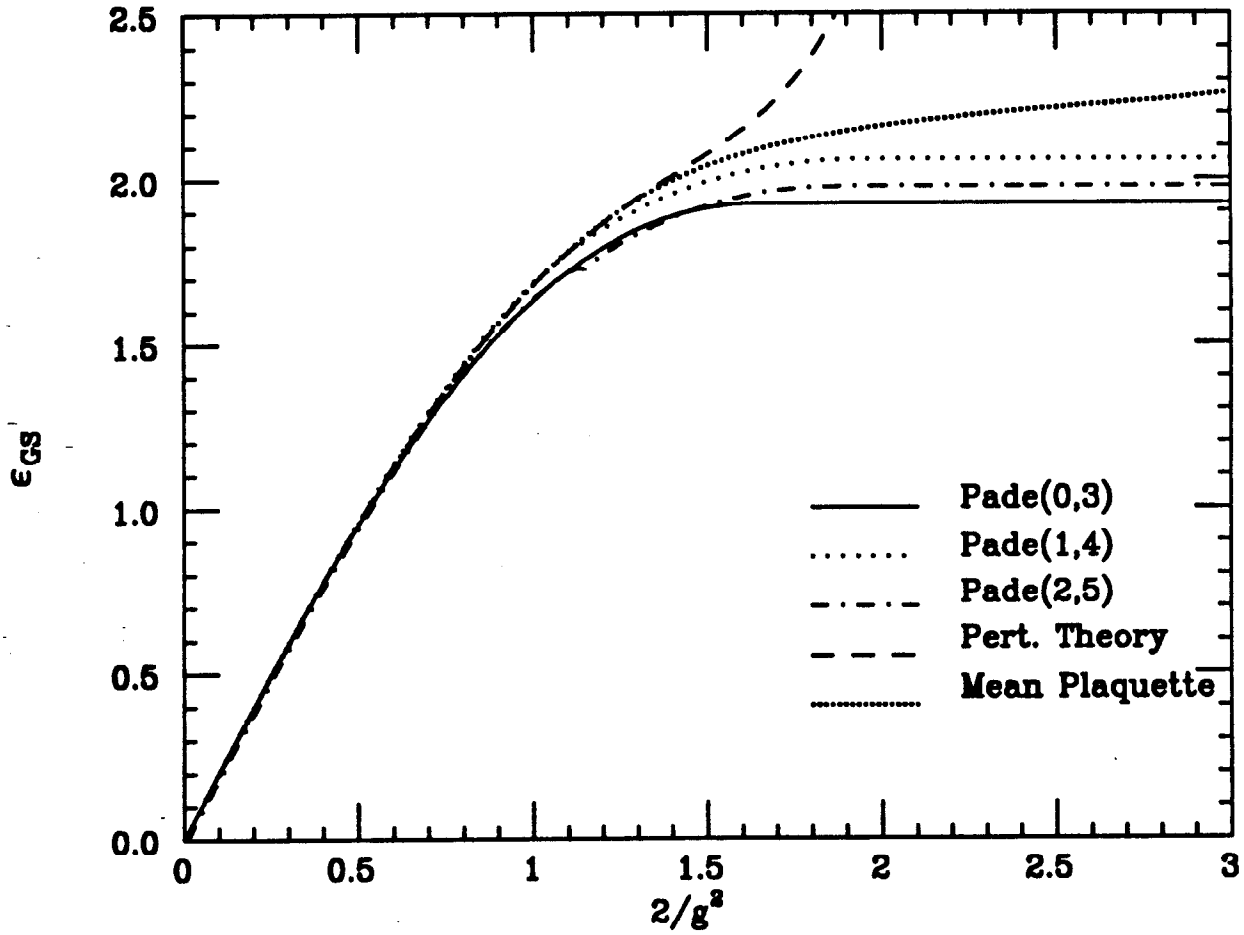
2.5
2.0
1.5
1.0
0.5
0.0
ϵ_{GS}
0
0.5
1
1.5
2
2.5
3
$2/g^2$
Pade(0,3)
Pade(1,4)
Pade(2,5)
Pert. Theory
Mean Plaquette

FIG. 2B

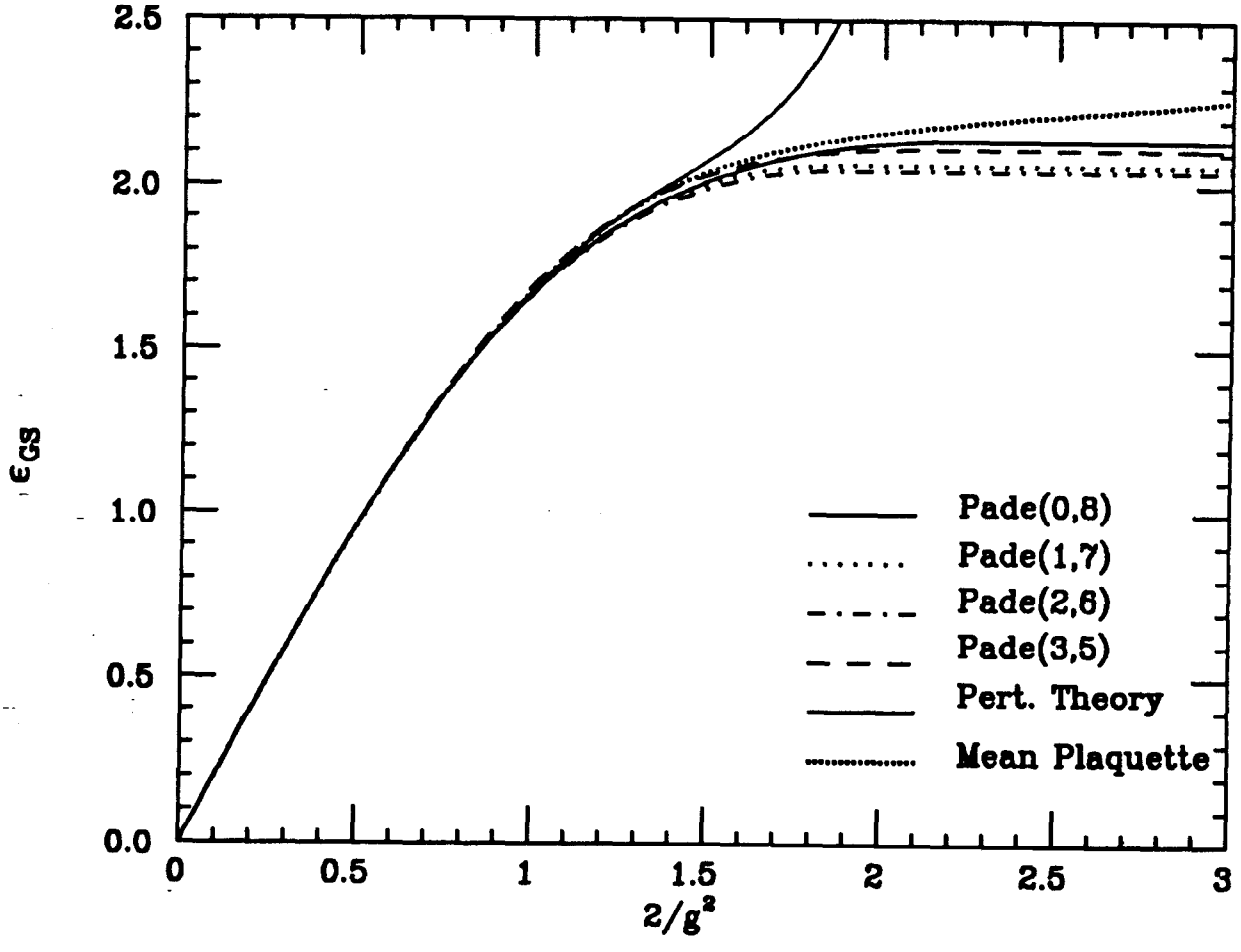
2.5
2.0
1.5
1.0
0.5
0.0
ϵ_{GS}
0
0.5
1
1.5
2
2.5
3
$2/g^2$
Pade(0,8)
Pade(1,7)
Pade(2,6)
Pade(3,5)
Pert. Theory
Mean Plaquette

FIG. 2C

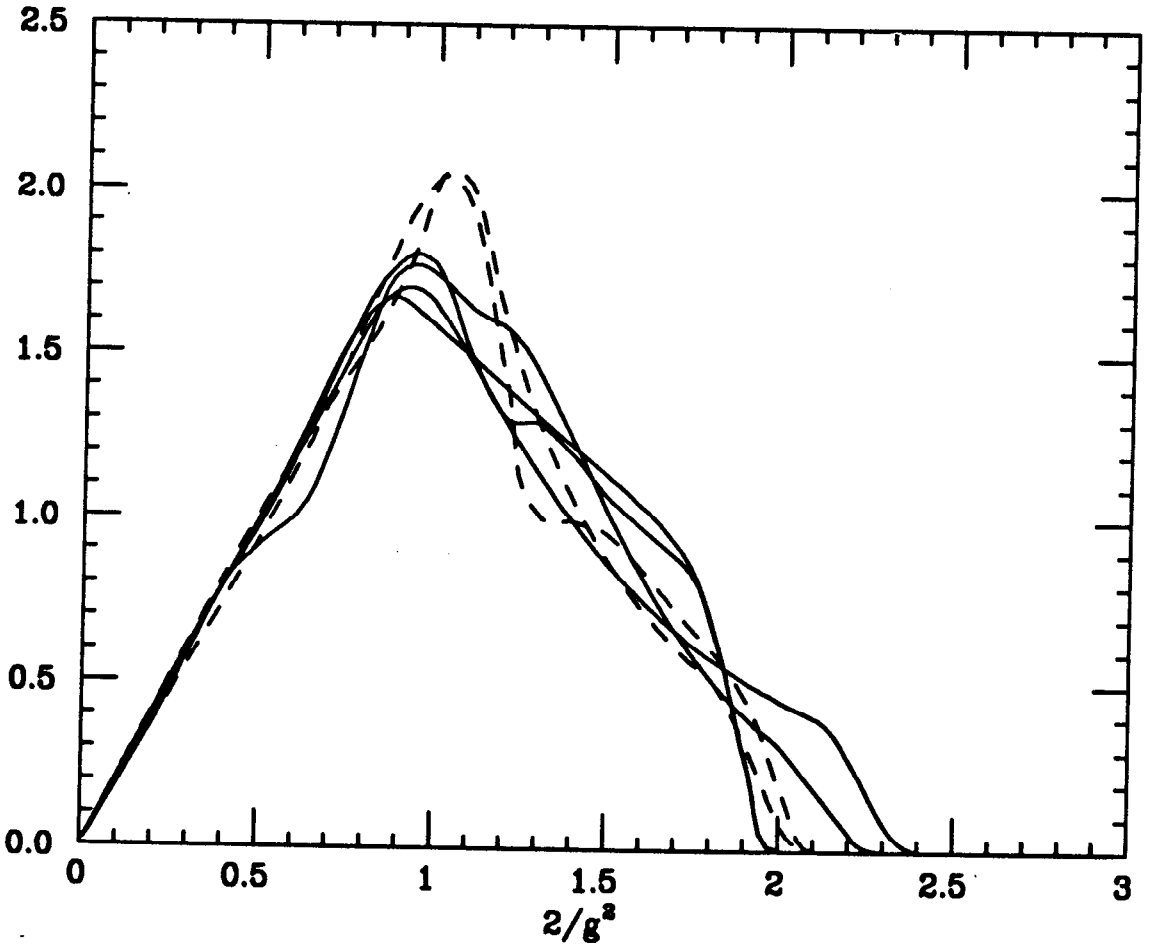

FIG. 3

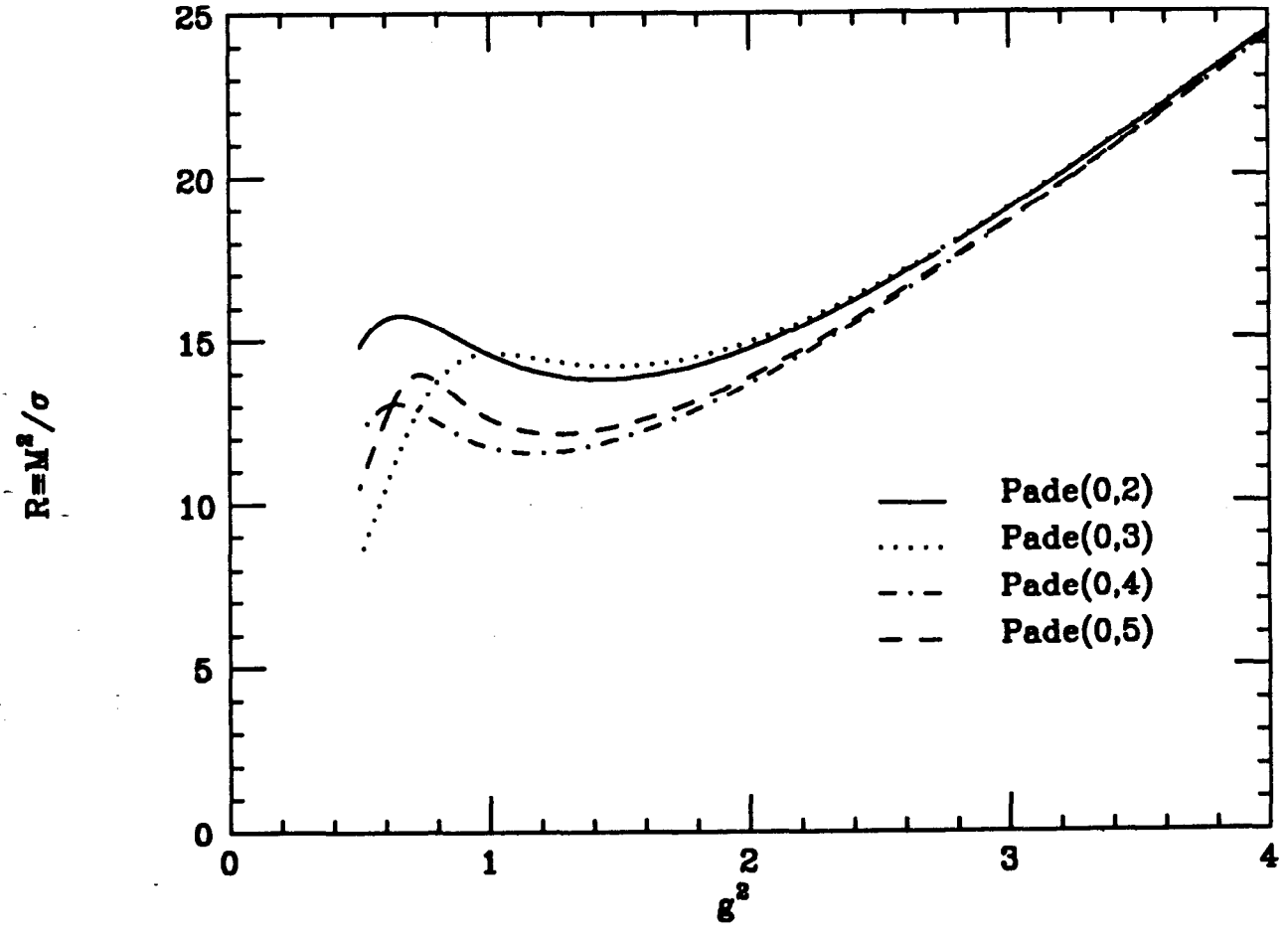

FIG. 4A

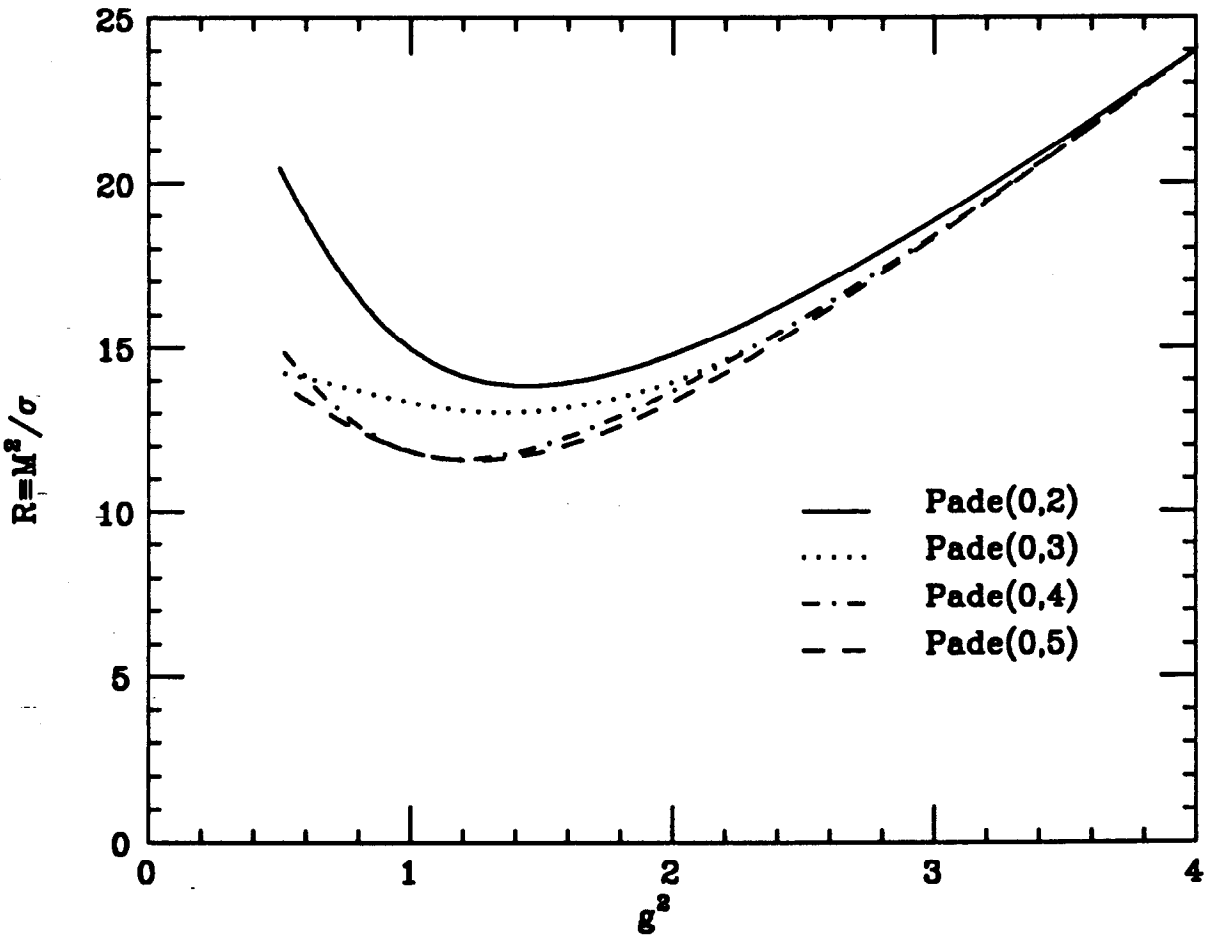

FIG. 4B

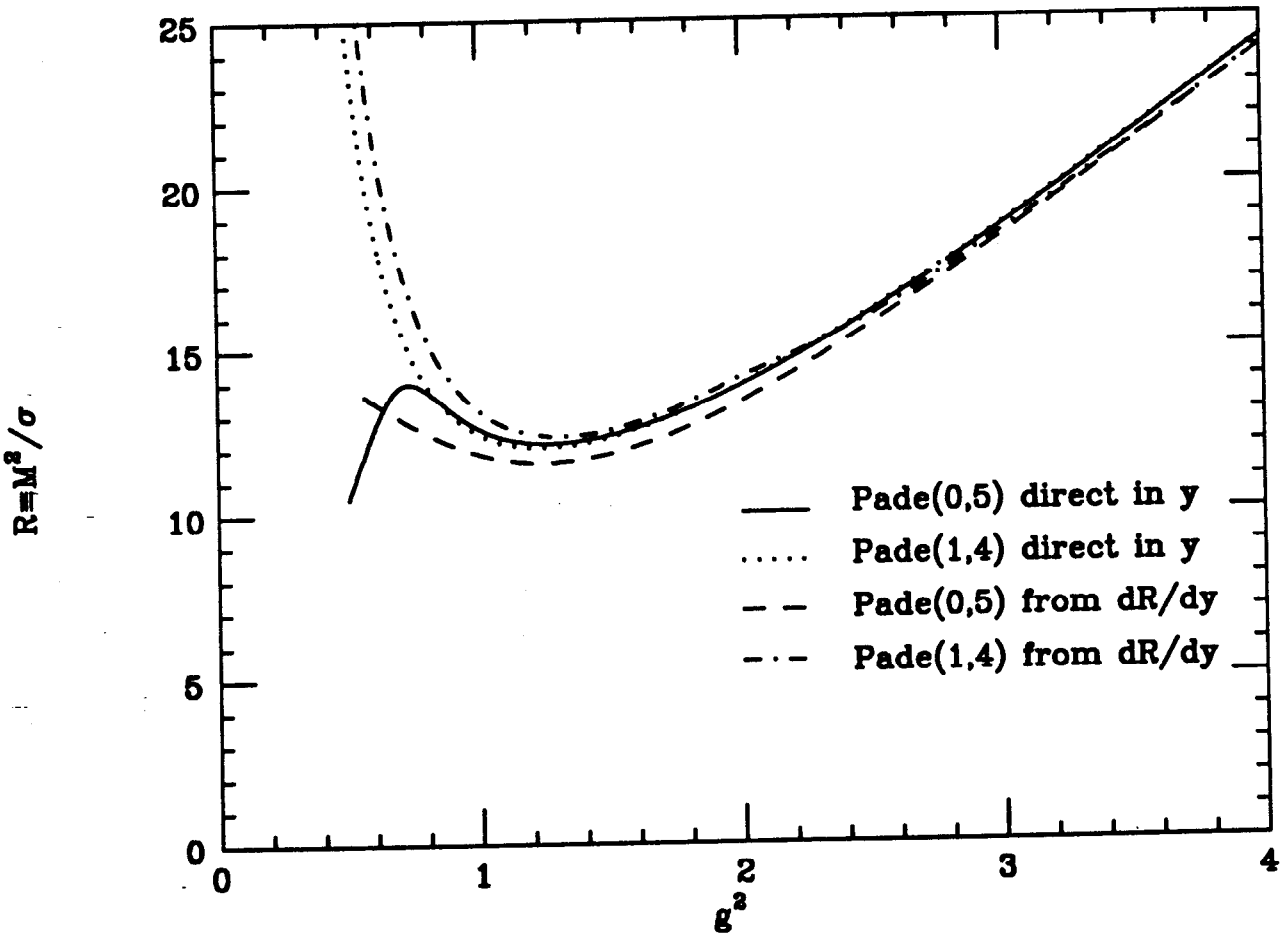
25
20
15
10
5
0
0
1
2
3
4
$R \equiv M^2/\sigma$
g^2
Pade(0,5) direct in y
Pade(1,4) direct in y
Pade(0,5) from dR/dy
Pade(1,4) from dR/dy

FIG. 4C

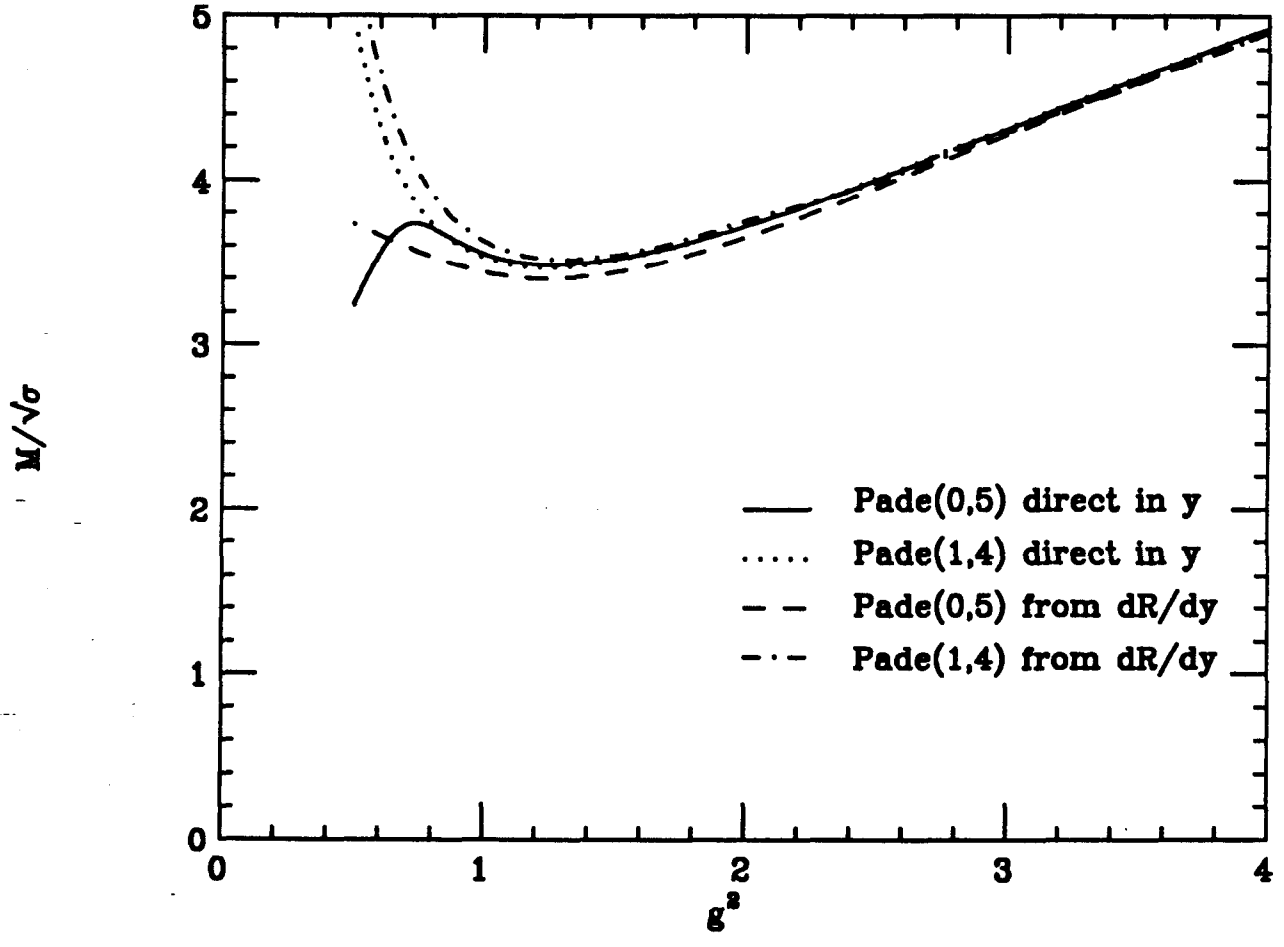
5
4
3
2
1
0
0
1
2
3
4
M/√σ
g²
Pade(0,5) direct in y
Pade(1,4) direct in y
Pade(0,5) from dR/dy
Pade(1,4) from dR/dy

FIG. 5

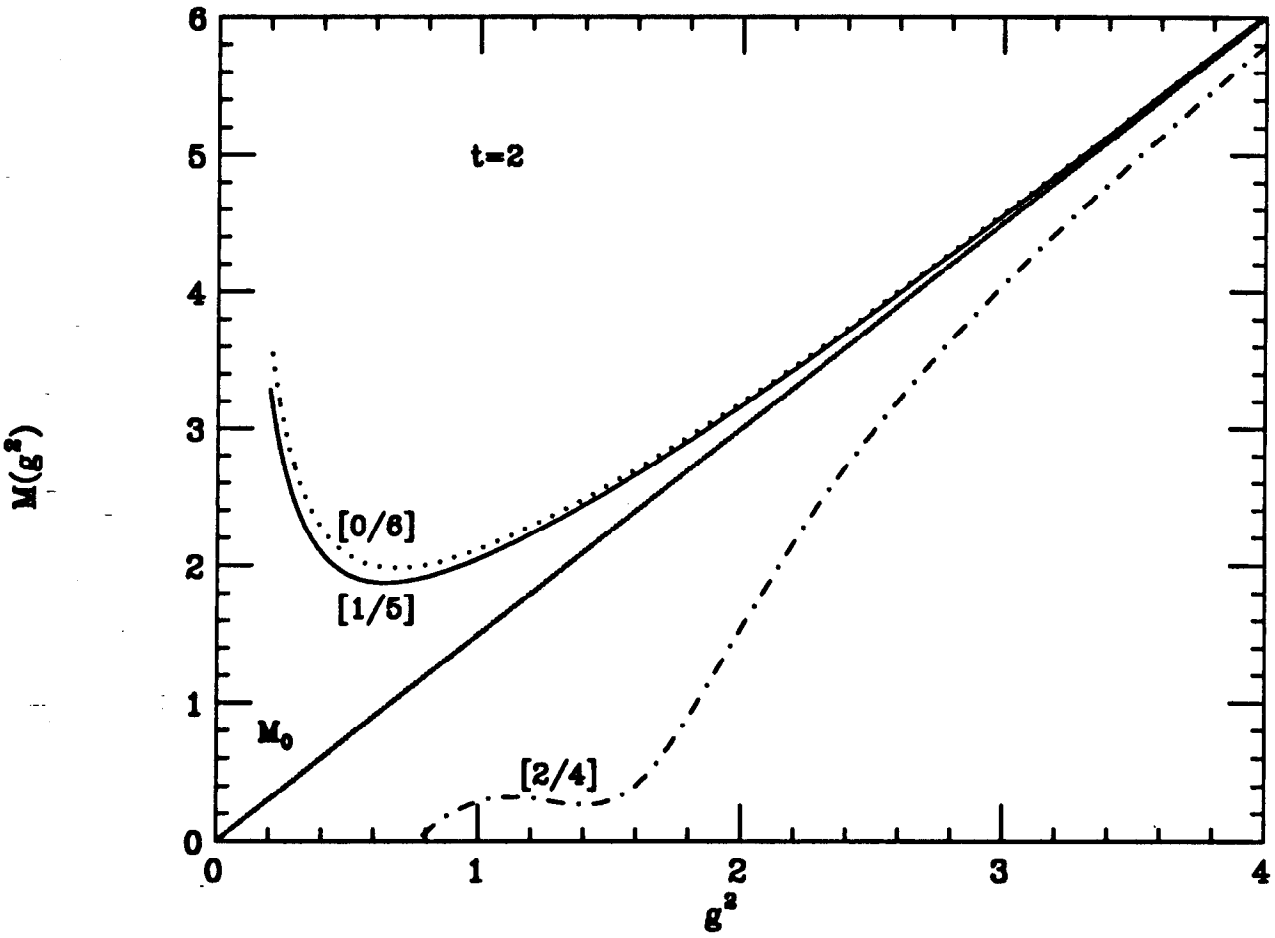

FIG. 6A

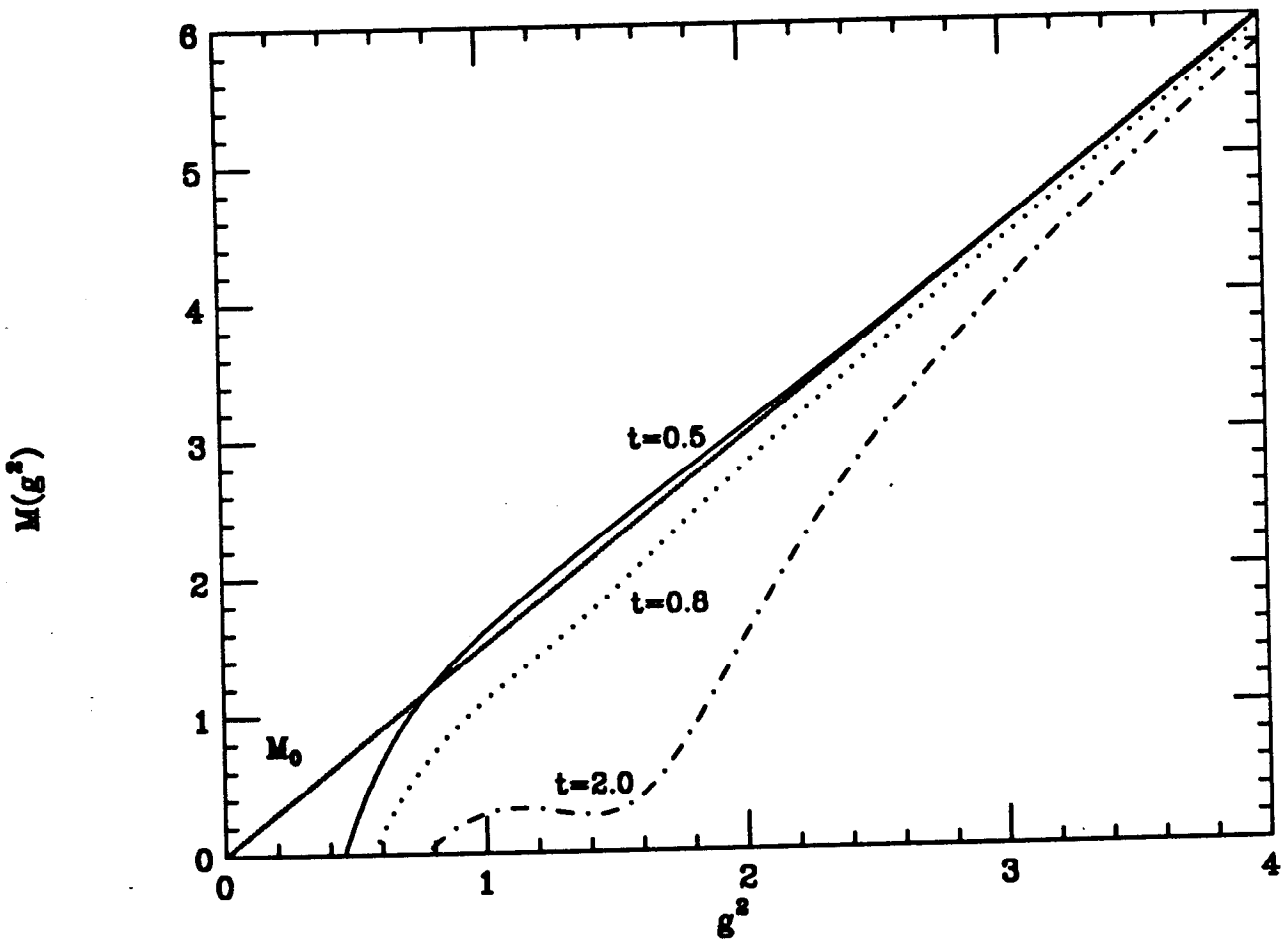

FIG. 6B

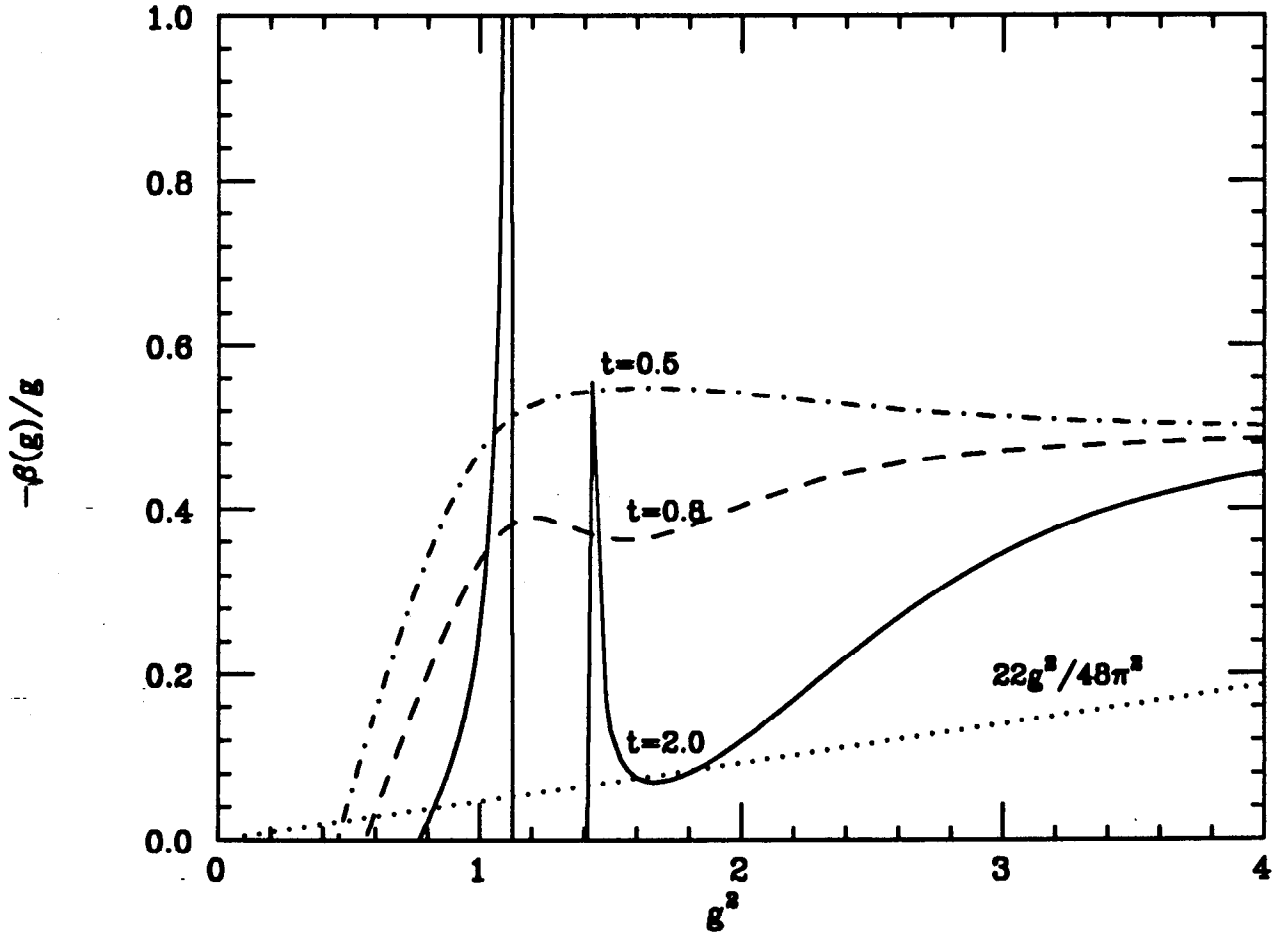

FIG. 7

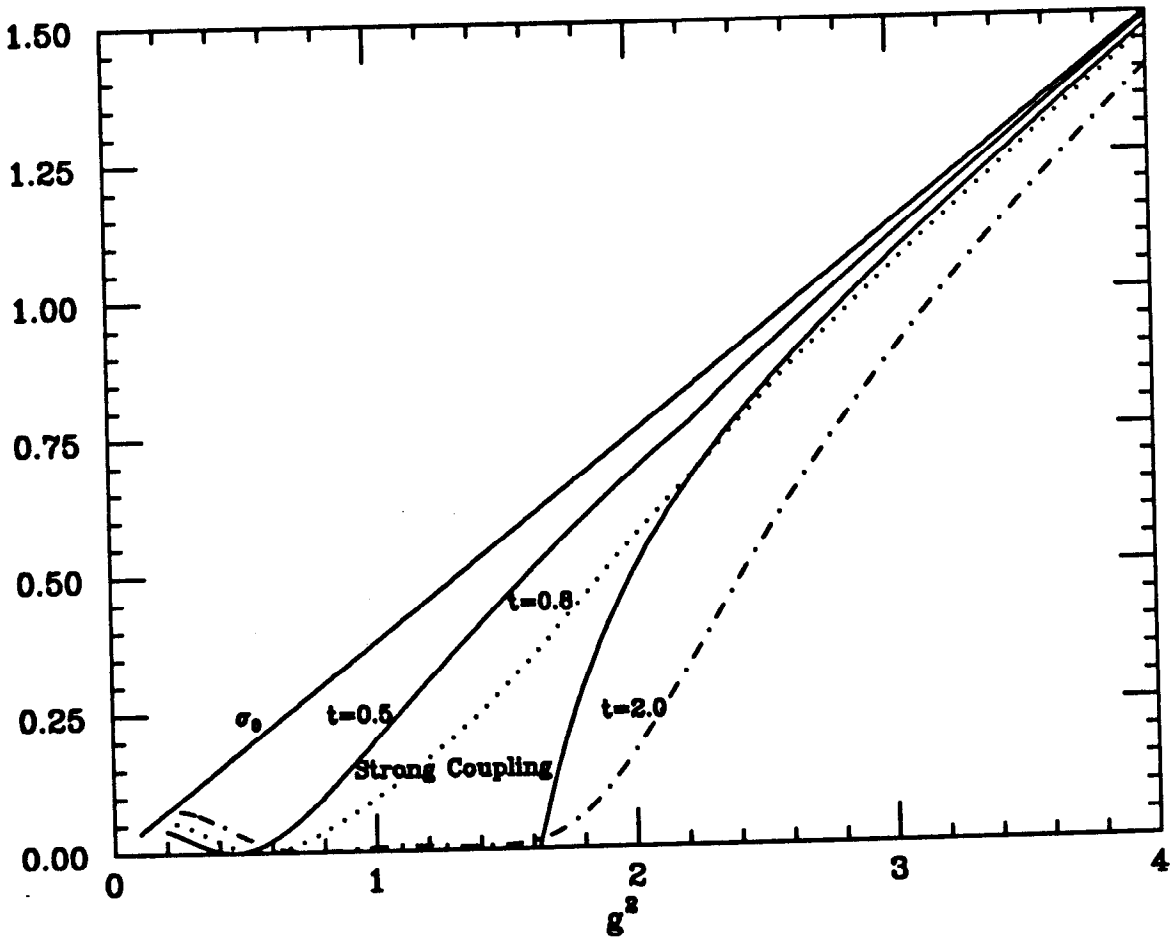
1.50
1.25
1.00
0.75
0.50
0.25
0.00
σ
0
1
2
3
4
g²
σ₀
t=0.5
t=0.8
t=2.0
Strong Coupling

FIG. 8

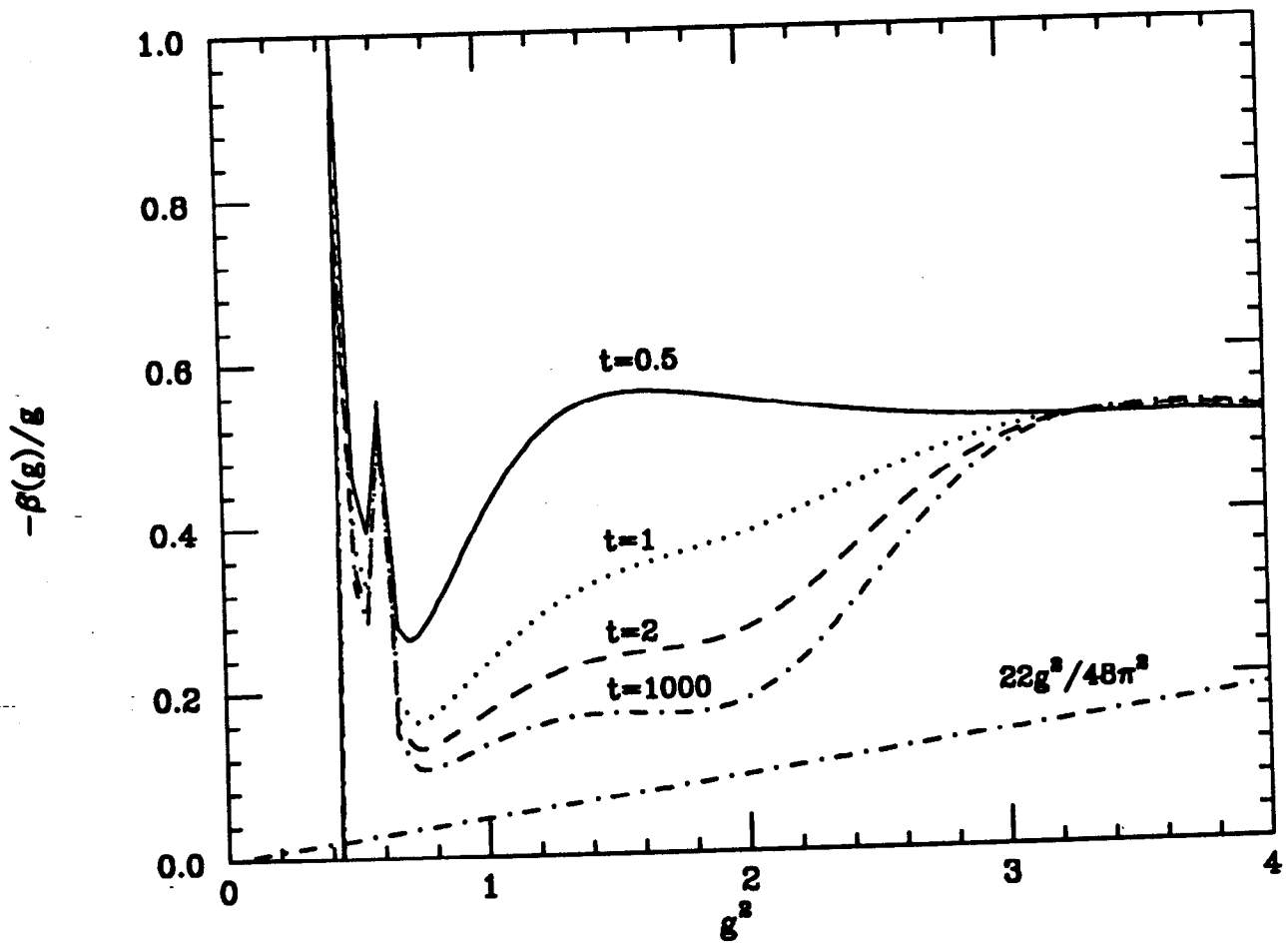

FIG. 9

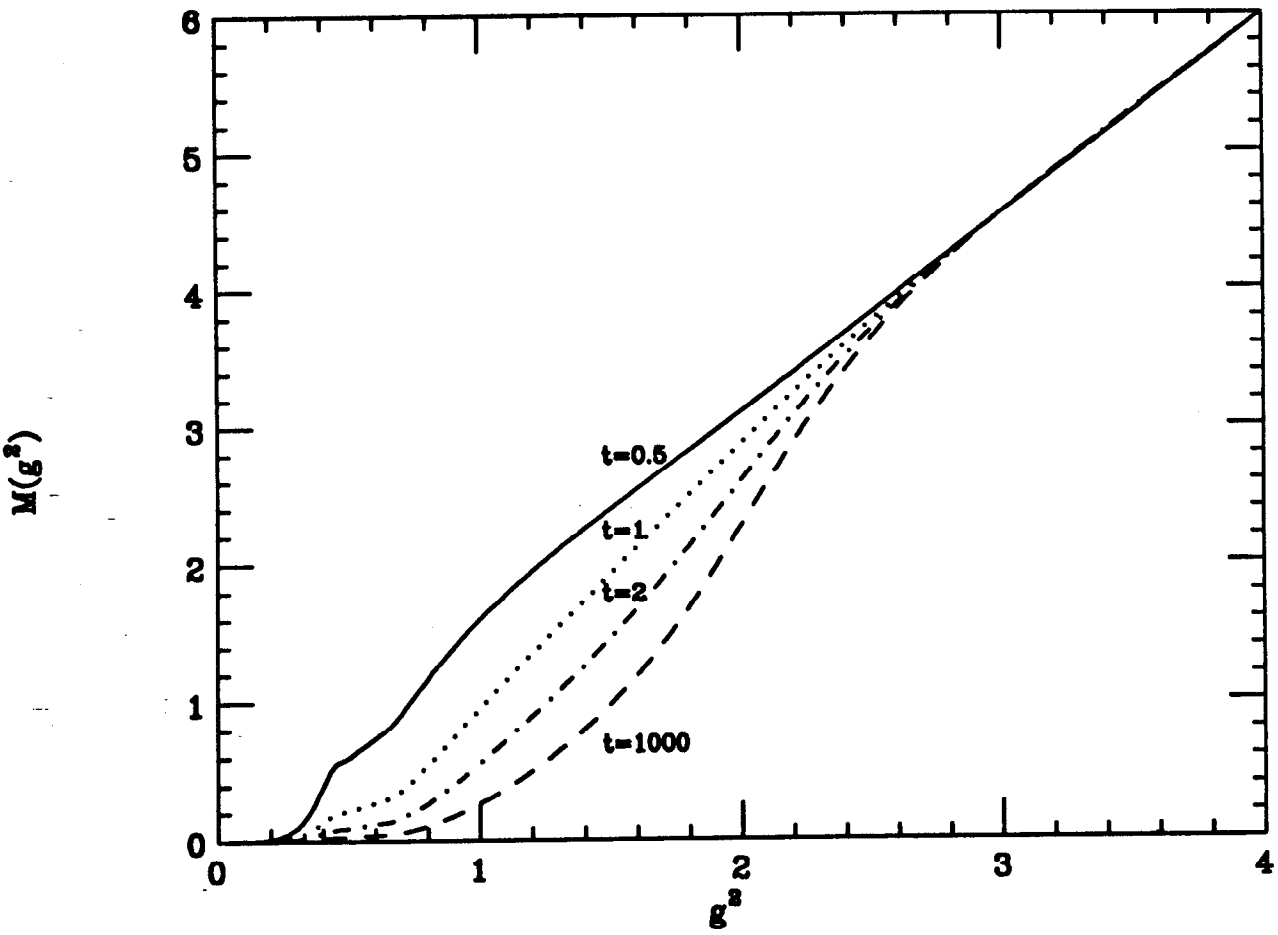

FIG. 10

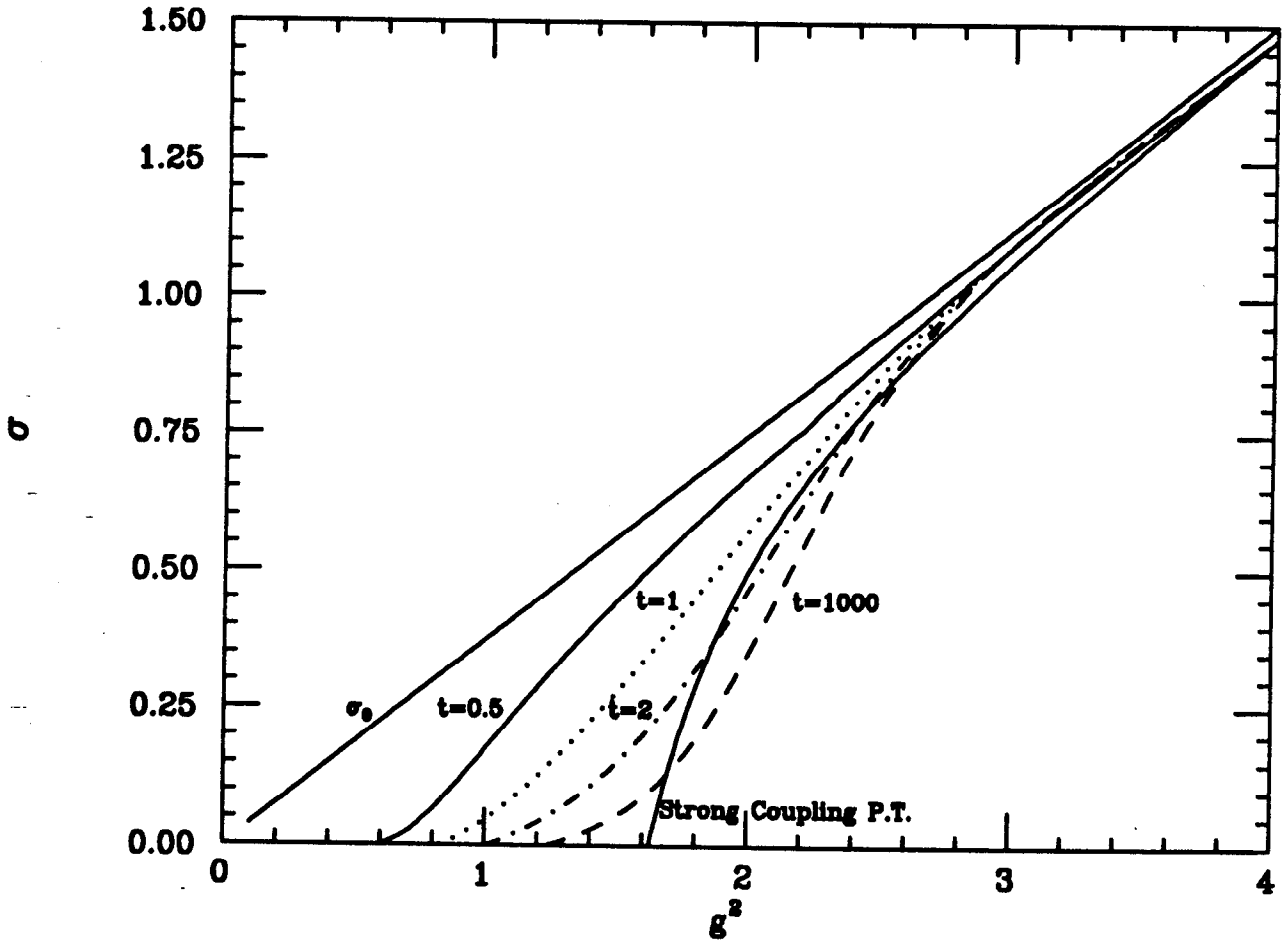
1.50
1.25
1.00
0.75
0.50
0.25
0.00
σ
0
1
2
3
4
g²
σ₀
t=0.5
t=1
t=2
t=1000
Strong Coupling P.T.

FIG. 11